

Stochastic Model Predictive Control with a Safety Guarantee for Automated Driving: Extended Version

Tim Brüdigam, Michael Olbrich, Dirk Wollherr, Marion Leibold

Abstract—Automated vehicles require efficient and safe planning to maneuver in uncertain environments. Largely this uncertainty is caused by other traffic participants, e.g., surrounding vehicles. Future motion of surrounding vehicles is often difficult to predict. Whereas robust control approaches achieve safe, yet conservative motion planning for automated vehicles, Stochastic Model Predictive Control (SMPC) provides efficient planning in the presence of uncertainty. Probabilistic constraints are applied to ensure that the maximal risk remains below a predefined level. However, safety cannot be ensured as probabilistic constraints may be violated, which is not acceptable for automated vehicles. Here, we propose an efficient trajectory planning framework with safety guarantees for automated vehicles. SMPC is applied to obtain efficient vehicle trajectories for a finite horizon. Based on the first optimized SMPC input, a guaranteed safe backup trajectory is planned using reachable sets. This backup is used to overwrite the SMPC input if necessary for safety. Recursive feasibility of the safe SMPC algorithm is proved. Highway simulations show the effectiveness of the proposed method regarding performance and safety.

Index Terms—model predictive control, stochastic model predictive control, failsafe trajectory planning, automated vehicles

I. INTRODUCTION

Within the past decades, research has made significant progress in the area of self-driving cars. Improvements in computer vision-based sensing and the use of this sensor data in control algorithms enable automated vehicles to detect and react to hazards in dynamic traffic and a constantly changing environment. A majority of road accidents is still caused by human errors, therefore, increasing the level of vehicle autonomy has great potential to reduce the overall number of accidents. Automated vehicles are especially relevant in critical situations where a significant number of human drivers is incapable of performing necessary maneuvers in time [1].

The safety of fully automated vehicles depends on the ability of the vehicle control algorithm to handle uncertainty of other traffic participants and the environment. While there are various control methods to plan vehicle trajectories, Model Predictive Control (MPC) has proved to be a suitable approach for automated vehicle trajectory planning [2], [3].

The authors gratefully acknowledge the financial and scientific support by the BMW Group.

T. Brüdigam, D. Wollherr, and M. Leibold are with the Chair of Automatic Control Engineering at the Technical University of Munich, Munich, Germany (email: {tim.brueDIGAM; dw; marion.leibold}@tum.de).

M. Olbrich is with the Department of Computer Science at the University of Augsburg, Augsburg, Germany (email: michael.olbrich@informatik.uni-augsburg.de).

MPC iteratively solves an optimal control problem on a finite prediction horizon, based on minimizing a cost function, while considering constraints on the vehicle input and state. Uncertainties in the prediction model are addressed by Robust Model Predictive Control (RMPC) [4].

RMPC approaches were designed for trajectory planning in automated vehicles [5], [6], however, robustly accounting for uncertainty yields conservative vehicle behavior. Conservatism resulting from robustly handling uncertainty in MPC is reduced by Stochastic Model Predictive Control (SMPC) [7], [8], where robust constraints are reformulated into probabilistic constraints. This probabilistic reformulation enables optimistic trajectory planning in a majority of scenarios, but it also allows a small probability of constraint violation, i.e., a probability of collision for vehicles. Various types of SMPC have been studied in the area of automated vehicles, showing the advantage of planning optimistic trajectories in a majority of scenarios [9], [10].

In comparison to SMPC, trajectory planning based on reachability analysis provides formal safety guarantees [11], [12]. Here, worst-case predictions are obtained for other surrounding vehicles in order to plan fail-safe vehicle trajectories, referred to as fail-safe trajectory planning (FTP), which is closely related to RMPC.

This paper is the extended version of [13]. In this work, we tackle the challenge of planning efficient and safe trajectories for automated vehicles. We present a novel MPC trajectory planner which combines the advantages of SMPC and fail-safe trajectory planning for environments with uncertainty. A trajectory is planned with SMPC, providing optimistic and efficient planning. In a regular setting, the first optimized SMPC input is then applied to the vehicle and a new SMPC optimal control problem is solved at the next time step with a shifted horizon. In addition to SMPC, for every time step a fail-safe trajectory is planned, given the first optimized SMPC input. The optimistic SMPC input is only applied to the vehicle if it is still possible to find a fail-safe backup trajectory after having applied the first SMPC input. This ensures that the efficient SMPC trajectory is executed as long as a backup exists, therefore guaranteeing safety. The proposed method is referred to as *Stochastic Model Predictive Control + fail-safe trajectory planning* (SMPC+FTP).

The contributions of this work are as follows.

- Novel SMPC+FTP method providing efficient and safe trajectory planning including lane change decisions.
- Elaborate case differentiation for safety constraints.
- Proof of recursive feasibility of the SMPC+FTP method.
- Simulation study with complex highway traffic situations.

We present the proposed SMPC+FTP approach in detail, ensuring safety for the vehicle while exploiting the benefits of efficient SMPC trajectory planning. The design of the SMPC+FTP method guarantees recursive feasibility, i.e., if a solution exists at a time step, it is guaranteed that a solution also exists at the next time step. This property is necessary to ensure safe trajectory planning with MPC. This extended version presents a detailed case differentiation to generate safety constraints with respect to other surrounding vehicles, both for the SMPC and the FTP optimal control problem. A simulation study of two complex scenarios demonstrates the benefits of optimistic trajectory planning in a regular highway scenario, while the ability of SMPC+FTP to guarantee safety is shown in an emergency scenario.

The paper is structured as follows. In Section I-A related work is presented. Then, the basics of SMPC and FTP are introduced in Section II, while the relevant vehicle models are presented in Section III. The proposed SMPC+FTP approach is derived in Section IV, and details for the respective SMPC and FTP optimal control problems are provided in Section V. The simulation results are presented in Section VI. A discussion and conclusive remarks are given in Section VII and Section VIII.

A. Related Work

Trajectory planning for automated vehicles is a widely studied research area. There are various methods in non-MPC related fields, such as using partially observable Markov decision processes (POMDP) [14] or reinforcement learning [15]. Learning based methods are also popular for autonomous racing [16]–[19]. When considering automated road vehicles, planning trajectories with MPC has the advantage of iteratively replanning the vehicle trajectory with constraints, accounting for a changing environment.

Standard MPC has been developed for cooperative adaptive cruise control, focusing on cooperative driving [20], [21]. MPC is also designed specifically to plan trajectories for a single autonomous vehicle [22] or for combined maneuver and trajectory planning [23]. MPC was also combined with potential-field methods in order to avoid static and dynamic obstacles [24].

The main focus of this work is trajectory planning with robust or stochastic MPC, as well as fail-safe trajectory planning (FTP). Fail-safe trajectory planning is defined as planning collision-free vehicle trajectories, accounting for any legal future motion of surrounding vehicles [25]. For bounded uncertainties in real-world applications, FTP is applied based on finding worst-case sets. Combined with reachability analysis, formal safety guarantees are given [12]. The computation of these reachable sets is connected to control invariant sets in RMPC as stated in [26]. An approach to include reachability analysis into MPC is given in [27].

In [28] a method is proposed to compute the set of all future locations possibly occupied by traffic participants. The remaining safe space is admissible to plan emergency trajectories. This FTP is presented in [11]. First, given the most likely motion of surrounding vehicles, an optimal trajectory is

determined. Then, an emergency trajectory is connected to the last point of the optimal trajectory for which collision avoidance is still guaranteed. The safe space is determined by an over-approximated set of any possible future vehicle motion. The fail-safe trajectory is generated in such a way that the controlled vehicle comes to a standstill. In [25] an FTP method is introduced which generates fail-safe trajectories in real-time. The method is tested in various simulations based on the CommonRoad benchmark framework [29]. A motion planning framework is introduced in [30] which combines reachability analysis with optimization-based trajectory planning. In [6] an RMPC method is suggested which uses a combination of a potential field like function and reachability sets to obtain safe zones on the road. A further RMPC method for collision avoidance with moving obstacles is presented in [5].

Stochastic Model Predictive Control (SMPC) has been intensively studied in the context of automated vehicles. These works focus on the trade-off between risk and conservatism, defined by probabilistic constraints, so called chance constraints [31]. On the one hand, taking into account unlikely uncertainty realizations drastically reduces efficacy, on the other hand, planning too optimistically increases risk. A major challenge in SMPC is reformulating the probabilistic chance constraint into a tractable constraint, which can be handled by a solver.

An SMPC particle approach is shown in [32] with a simple vehicle braking scenario, where particles approximate the uncertainty. An SMPC trajectory planner for automated vehicles in the presence of fixed obstacles is presented in [33]. In [9] the environment is modeled by an Interacting Multiple Model Kalman filter. Given the most likely prediction for surrounding vehicles, a vehicle trajectory is then planned with SMPC assuming Gaussian uncertainty. Varying risk parameters, denoting the level of accepted risk, are studied, illustrating the trade-off between risk and conservatism. In [34] an SMPC lane change controller is presented, where the lane change risk is considered using predicted time-to-collision.

A different SMPC approach is utilized in [10], [35], focusing on Scenario Stochastic Model Predictive Control (SCMPC) based on [36], [37]. In SCMPC samples of the uncertainty are drawn, which must then satisfy the constraints to find a tractable chance constraint expression. Arbitrary probability distributions are handled by SCMPC, while standard SMPC usually requires Gaussian distributions to analytically reformulate the chance constraint. While [35] focuses on simple lane change scenarios, the work is extended in [10] and experimental results are presented.

A combination of SMPC and SCMPC is given in [38], exploiting the individual advantages of SMPC and SCMPC. SCMPC is used to cope with maneuver uncertainty of surrounding vehicles, while SMPC addresses the maneuver execution uncertainty, described by a Gaussian probability distribution. A further approach to SMPC is presented in [39], where a grid-based SMPC method is applied to plan vehicle trajectories, based on occupancy grids [40], [41].

In summary, SMPC approaches provide efficient vehicle trajectories for the majority of uncertainty realizations in regular situations. However, for unlikely uncertainty realizations,

safety issues occur.

In this work, the benefit of efficiently planning trajectories with SMPC is combined with the safety guarantee of FTP. The FTP in this work is inspired by the ideas of [11], [25], [28]. In the following, SMPC and FTP are introduced. Then the proposed SMPC+FTP method is derived in detail.

B. Notation

Regular letters denote scalars, bold lowercase letters indicate vectors, and bold uppercase letters are used for matrices, e.g., a , \mathbf{a} , \mathbf{A} , respectively. The Euclidean norm is denoted by $\|\cdot\|_2$ and $\|\mathbf{z}\|_{\mathbf{Z}} = \mathbf{z}^\top \mathbf{Z} \mathbf{z}$. The probability of an event is given by $\Pr(\cdot)$. The state at time step h is denoted by \mathbf{x}_h . For MPC optimal control problems the prediction step k is used, i.e., \mathbf{x}_k . If clear from context, the time step h is not specifically mentioned in the context of optimal control problems due to clarity. Estimated states are indicated by $\hat{\mathbf{x}}$.

II. PRELIMINARIES

In the following we briefly introduce the general MPC optimal control problems for SMPC and FTP in safety-critical applications. Details on SMPC and FTP, which are relevant for application in automated driving, are then given in Section V-A and Section V-B, respectively.

MPC iteratively solves an optimal control problem (OCP) with a finite prediction horizon N subject to input and state constraints. After solving the MPC optimal control problem, only the first input \mathbf{u}_0 of the optimized input sequence $\mathbf{U} = (\mathbf{u}_0, \dots, \mathbf{u}_{N-1})^\top$ is applied. At the next time step the updated MPC optimal control problem is solved again. We distinguish between regular time steps h and prediction steps k within the MPC OCP. If clear from context, the time step h is not specifically mentioned. In the following we only explicitly denote the prediction time step k . The current time step h , at which the MPC optimal control problem is computed, is omitted to improve clarity.

A. SMPC with Chance Constraints

While standard MPC considers hard constraints, this is problematic if uncertainties are present. Avoiding the worst-case realizations for uncertainties results in an overly conservative solution of the optimal control problem, which is unfavorable for automated driving. Hard constraints subject to uncertainty can be considered by chance constraints. This yields the SMPC optimal control problem

$$V^* = \min_{\mathbf{U}} \sum_{k=0}^{N-1} l(\xi_k, \mathbf{u}_k) + V_f(\xi_N) \quad (1a)$$

$$\text{s.t. } \xi_{k+1} = \mathbf{f}(\xi_k, \mathbf{u}_k) \quad (1b)$$

$$\xi_k \in \Xi_k \quad \forall k \in \{1, \dots, N\}, \quad (1c)$$

$$\mathbf{u}_k \in \mathcal{U}_k \quad \forall k \in \{0, \dots, N-1\}, \quad (1d)$$

$$\Pr(\xi_k \in \Xi'_{k,\text{safe}}(\mathbf{w})) \geq \beta \quad \forall k \in \{1, \dots, N\} \quad (1e)$$

with prediction step k , states ξ_k , input sequence $\mathbf{U} = [\mathbf{u}_0, \mathbf{u}_1, \dots, \mathbf{u}_{N-1}]^\top$, system dynamics \mathbf{f} , and the normally distributed, zero mean uncertainty $\mathbf{w} \sim \mathcal{N}(\mathbf{0}, \Sigma^w)$ with

covariance matrix Σ^w . The cost function consists of the stage cost $l(\xi_k, \mathbf{u}_k)$ and the terminal cost $V_f(\xi_N)$. States and inputs are bounded by the state and input constraint sets Ξ_k and \mathcal{U}_k , respectively, and the safety constraint $\Xi'_{k,\text{safe}}(\mathbf{w})$ depends on the uncertainty \mathbf{w} . The probabilistic chance constraint is given by (1e). The safety constraint $\xi_k \in \Xi'_{k,\text{safe}}(\mathbf{w})$ is required to hold according to the risk parameter β , i.e., the probability of $\xi_k \in \Xi'_{k,\text{safe}}(\mathbf{w})$ must be larger for a larger risk parameter β . For $\beta < 1$ a certain constraint violation probability is therefore allowed.

The chance constraint (1e) cannot be handled by a solver directly, but is required to be reformulated into a deterministic expression. Details on the reformulation are given in Section V-A.

In this work, uncertainty is considered regarding surrounding vehicles. The safe set $\Xi'_{\text{safe}}(\mathbf{w})$ therefore depends on how the uncertainty \mathbf{w} affects the surrounding vehicles. This is described in Section III. Note that SMPC optimal control problems can consider an expectation value in the cost function, however, this is omitted here as no expectation value will be necessary for the automated driving optimal control problem, i.e., the system dynamics (1b) do not include uncertainty. In the simulation study in Section VI the uncertainty in the safe set $\Xi'_{k,\text{safe}}(\mathbf{w})$ is governed by uncertainty in the behavior of surrounding vehicles.

B. Fail-safe Trajectory Planning

We also consider an MPC optimal control problem for FTP, i.e., a fail-safe MPC OCP. In contrast to SMPC, FTP considers the worst-case realizations of the uncertainty, resulting in safe, yet conservative optimized inputs. The FTP optimal control problem is given by

$$V^* = \min_{\mathbf{U}} \sum_{k=0}^{N-1} l(\xi_k, \mathbf{u}_k) + V_f(\xi_N) \quad (2a)$$

$$\text{s.t. } \xi_{k+1} = \mathbf{f}(\xi_k, \mathbf{u}_k) \quad (2b)$$

$$\xi_k \in \Xi_k \quad \forall k \in \{1, \dots, N\}, \quad (2c)$$

$$\mathbf{u}_k \in \mathcal{U}_k \quad \forall k \in \{0, \dots, N-1\}, \quad (2d)$$

$$\xi_k \in \Xi_{k,\text{safe}}(\mathbf{w}) \quad \forall k \in \{1, \dots, N-1\} \quad (2e)$$

$$\xi_N \in \Xi_{N,\text{safe}}(\mathbf{w}) \quad (2f)$$

which is similar to the SMPC problem (1). However, the safety constraint (2e) is not a chance constraint, as in (1e), but a hard constraint. In contrast to SMPC, for FTP the safe set $\Xi_{k,\text{safe}}(\mathbf{w})$ is constructed based on reachability analysis to ensure formal safety guarantees. This is strongly connected to the computation of invariant sets in RMPC. In addition to constraint (2e), a terminal constraint (2f) is required, which ensures that the terminal prediction state ξ_N allows to remain in a safe state beyond the prediction horizon. Based on this safe terminal set $\Xi_{N,\text{safe}}(\mathbf{w})$ it is guaranteed that there exist system inputs \mathbf{u}_{k+} with $k^+ > N$ resulting in safe states ξ_{k+} . Note that the safe set $\Xi'_{k,\text{safe}}(\mathbf{w})$ in (1e) is not necessarily computed in the same way as the safe set $\Xi_{k,\text{safe}}(\mathbf{w})$ in (2e),(2f). Details on the FTP optimal control problem are provided in Section V-B.

III. VEHICLE MODELS

MPC requires a system model for the controlled vehicle, known as the ego vehicle (EV), and surrounding vehicles, referred to as target vehicles (TVs), in order to predict future states within the optimal control problem.

A. Ego Vehicle Model

We use a kinematic bicycle model to predict the EV states on a finite horizon, as suggested in [42]. The continuous-time system is given by

$$\dot{s} = v \cos(\phi + \alpha), \quad (3a)$$

$$\dot{d} = v \sin(\phi + \alpha), \quad (3b)$$

$$\dot{\phi} = \frac{v}{l_r} \sin \alpha, \quad (3c)$$

$$\dot{v} = a, \quad (3d)$$

$$\alpha = \arctan \left(\frac{l_r}{l_r + l_f} \tan \delta \right), \quad (3e)$$

where l_r and l_f are the distances from the vehicle center of gravity to the rear and front axles, respectively. The state vector is $\xi = [s, d, \phi, v]^\top$ and the input vector is $u = [a, \delta]^\top$. The vehicle velocity is given by v , acceleration and steering angle are denoted by a and δ , respectively. We consider the longitudinal position s of the vehicle along the road, the lateral vehicle deviation d from the centerline of the right lane, and the orientation ϕ of the vehicle with respect to the road. The nonlinear vehicle model (3) is summarized as $\dot{\xi} = f^c(\xi, u)$.

Each MPC optimal control problem is initialized with a linearization of the nonlinear prediction model (3) around the current vehicle state $\xi^* = \xi_0$ and the input $u^* = [0, 0]^\top$. Selecting a non-zero reference input u^* often results in large differences $\Delta u = u_k - u^*$ for prediction steps far ahead, increasing the inaccuracy of the linearization. The linearized continuous-time vehicle model is then given by

$$\dot{\xi}^* + \Delta \dot{\xi} = f^c(\xi^*, 0) + A_1(\xi - \xi^*) + B_1 u \quad (4)$$

with the Jacobi matrices

$$A_1 = \left[\frac{\partial f^c}{\partial \xi} \right] \bigg|_{(\xi^*, u^*)}, \quad B_1 = \left[\frac{\partial f^c}{\partial u} \right] \bigg|_{(\xi^*, u^*)}. \quad (5)$$

A discrete-time model is required for MPC, therefore the linearized prediction model (4) is discretized with sampling time T . This yields the discrete states $\xi_k = [s_k, d_k, \phi_k, v_k]^\top$ and inputs $u_k = [a_k, \delta_k]^\top$ for prediction step k , as well as the linearized, discretized system

$$\xi_{k+1} = \xi_0 + T f^c(\xi_0, 0) + A_d(\xi_k - \xi_0) + B_d u_k \quad (6a)$$

$$= f^d(\xi_0, \xi_k, u_k) \quad (6b)$$

where A_d and B_d are matrices of the linearized system obtained from A_1, B_1 with zero-order hold. The nonlinear term $f^c(\xi^*, u^*)$ in (4) is approximated by a forward Euler method since ξ_0 is known. The linearized, discretized matrices A_d and B_d are given in Appendix A. In the following, for $k = 0$ in (6), i.e., $\xi_k = \xi_0$, the argument ξ_0 is only mentioned once, i.e., $f^d(\xi_0, \xi_0, u_0)$ is abbreviated as $f^d(\xi_0, u_0)$.

The following sections derive an SMPC method and constraints to avoid collisions with surrounding vehicles. However, even if no other vehicles are present, certain constraints are required. Acceleration and steering angle are bounded by

$$u_{\min} \leq u_k \leq u_{\max} \quad (7a)$$

$$\Delta u_{\min} \leq \Delta u_k \leq \Delta u_{\max} \quad (7b)$$

with $\Delta u_{k+1} = u_{k+1} - u_k$ and $u_{\max} = [a_{\max}, \delta_{\max}]^\top$, $u_{\min} = [a_{\min}, \delta_{\min}]^\top$. Further, road and velocity constraints are considered, resulting in

$$d_k \in \mathcal{D}^{\text{lane}} \quad (8a)$$

$$0 \leq v_k \leq v_{\max} \quad (8b)$$

where $\mathcal{D}^{\text{lane}}$ represents road boundaries and v_{\max} is the maximal velocity. Negative velocities are not allowed, i.e., $v_k \geq 0$.

In the following we refer to input constraints by the set of admissible inputs \mathcal{U} and state constraints are denoted by the set of admissible states Ξ .

B. Target Vehicle Model

In order to avoid collisions, the EV is also required to predict the future states of surrounding TVs. The prediction model for the TVs used by the EV is a linear, discrete-time point-mass model given by

$$\xi_{k+1}^{\text{TV}} = A \xi_k^{\text{TV}} + B u_k^{\text{TV}} \quad (9a)$$

$$u_k^{\text{TV}} = \tilde{u}_k^{\text{TV}} + w_k^{\text{TV}} \quad (9b)$$

where $\xi_k^{\text{TV}} = [x_k^{\text{TV}}, v_{x,k}^{\text{TV}}, y_k^{\text{TV}}, v_{y,k}^{\text{TV}}]^\top$ is the TV state with longitudinal position and velocity $x_k^{\text{TV}}, v_{x,k}^{\text{TV}}$ and lateral position and velocity $y_k^{\text{TV}}, v_{y,k}^{\text{TV}}$. The linear TV model allows to propagate the uncertainty, which is necessary for the MPC approach in the following sections. The TV model used in this work is only one possible option. Other linear TV prediction models can be utilized.

The system and input matrices are

$$A = \begin{bmatrix} 1 & T & 0 & 0 \\ 0 & 1 & 0 & 0 \\ 0 & 0 & 1 & T \\ 0 & 0 & 0 & 1 \end{bmatrix}, \quad B = \begin{bmatrix} 0.5T^2 & 0 \\ T & 0 \\ 0 & 0.5T^2 \\ 0 & T \end{bmatrix} \quad (10)$$

with sampling time T . The TV input consists of a feedback controller \tilde{u}_k^{TV} and a perturbation on the input, which is assumed to be an independent, identically distributed disturbance vector w_k^{TV} . This setup assumes that the TV is following a given reference while deviations are allowed. The TV feedback controller is given by

$$\tilde{u}_k^{\text{TV}} = K(\xi_k^{\text{TV}} - \xi_{\text{ref},k}^{\text{TV}}), \quad (11a)$$

$$K = \begin{bmatrix} 0 & k_{12} & 0 & 0 \\ 0 & 0 & k_{21} & k_{22} \end{bmatrix} \quad (11b)$$

with the TV reference $\xi_{\text{ref},k}^{\text{TV}}$. The feedback matrix K is obtained by a linear quadratic control strategy. As we assume that the TV follows a reference velocity in x -direction instead of reference x -positions, the TV input does not need to directly affect x_k^{TV} . The state x_k^{TV} is only used as a measured quantity. If the TV input computed by (11a) exceeds the

limits $\mathbf{u}_{\max}^{\text{TV}} = [a_{\max}, a_{y,\max}]^\top$ and $\mathbf{u}_{\min}^{\text{TV}} = [a_{\min}, a_{y,\min}]^\top$, summarized as \mathcal{U}^{TV} , the TV inputs are bounded to satisfy \mathcal{U}^{TV} .

We assume that \mathbf{w}_k^{TV} is subject to a Gaussian distribution with zero mean and covariance matrix $\Sigma_{\mathbf{w}}^{\text{TV}}$, which is denoted by $\mathbf{w}_k^{\text{TV}} \sim \mathcal{N}(0, \Sigma_{\mathbf{w}}^{\text{TV}})$. We also consider sensor noise in the measurement of the TV state, i.e.,

$$\hat{\xi}_0^{\text{TV}} = \xi_0^{\text{TV}} + \mathbf{w}_0^{\text{sens}} \quad (12)$$

where $\hat{\xi}_0^{\text{TV}}$ is the measured initial state of the TV by the EV. The sensor noise $\mathbf{w}_0^{\text{sens}} = [w_{0,x}^{\text{sens}}, w_{0,v_x}^{\text{sens}}, w_{0,y}^{\text{sens}}, w_{0,v_y}^{\text{sens}}]^\top$ is assumed to be a truncated Gaussian noise with $\mathbf{w}_0^{\text{sens}} \sim \mathcal{N}(0, \Sigma^{\text{sens}})$ and $\mathbf{w}_0^{\text{sens}} \in \mathcal{W}^{\text{sens}}$, where $\mathcal{W}^{\text{sens}}$ is a compact, convex and bounded set.

IV. STOCHASTIC MODEL PREDICTIVE CONTROL WITH SAFETY GUARANTEE

SMPC and fail-safe trajectory planning both have their individual advantages, i.e., efficient trajectories in an uncertain environment and guaranteed safe motion planning, respectively. However, both methods come with certain disadvantages. SMPC allows a predefined probability of constraint violation and thus potentially collisions, while FTP can result in overly conservative trajectories. In the following we will present a combined SMPC and FTP framework, SMPC+FTP, which exploits advantages of both methods to enable efficient and safe trajectories for autonomous vehicles. This section introduces the general setup of the SMPC+FTP framework and gives a proof for recursive feasibility. The subsequent Sections V-A and V-B provide details on the individual SMPC and FTP algorithms, respectively, which are required for the combined SMPC+FTP approach.

A. SMPC+FTP Method

Before presenting the SMPC+FTP method, we need to define requirements for a safe ego vehicle state as well as a safe input sequence $\mathbf{U}_{\text{safe}} = [\mathbf{u}_{\text{safe},0}, \mathbf{u}_{\text{safe},1}, \dots, \mathbf{u}_{\text{safe},m}]^\top$ with $m+1$ individual inputs. Note that m is not directly related to the MPC prediction horizon.

Definition 1 (Safe State). *The state of an ego vehicle, fully located in one lane, is considered to be safe if there is no lateral vehicle motion, i.e., $\phi = 0$, and if the ego vehicle velocity is lower than the velocity of the target vehicle in front on the same lane (or if the ego vehicle velocity is zero). The set of safe states is indicated by Ξ_{safe} .*

Definition 2 (Safe Input Sequence). *An input sequence \mathbf{U}_{safe} is considered safe if consecutively applying all elements of \mathbf{U}_{safe} results in a state trajectory that avoids collisions and eventually leads to zero velocity.*

The definition of safe states and safe input sequences results in assumptions for TVs.

Assumption 1 (Traffic Rules). *The target vehicles adhere to the traffic rules that are assumed for the prediction of future target vehicle behavior.*

Assumption 2 (Vehicle Deceleration). *The maximum absolute value of the ego vehicle deceleration is at least as large as the maximum absolute value of the target vehicle deceleration.*

Given a safe EV state, there exists a safe input sequence \mathbf{U}_{safe} , consisting of deceleration and zero steering, which results in an EV zero velocity state in the current EV lane, i.e., zero velocity in x -direction and y -direction. This is based on the assumptions that the other TVs adhere to traffic rules and that the TV deceleration is not larger than the EV deceleration. TVs behaving against traffic rules cannot be reliably accounted for by any prediction and the deceleration assumption is necessary to avoid colliding with a braking TV in front.

In the following we focus on the SMPC+FTP optimal control problems which are solved at each time step h . Within the OCP only the prediction steps k are relevant. For clarity we therefore omit explicitly denoting the current time step h in the following. Within the OCP the current EV state at time step h and prediction step $k=0$ is denoted by ξ_0 .

At the initialization of each OCP, the current EV state ξ_0 and the current TV state ξ_0^{TV} are known to the EV. Additionally, a safe input sequence \mathbf{U}_{safe} is available from the SMPC+FTP problem solved at the previous time step. Later we will focus on obtaining a safe input sequence for the SMPC+FTP iteration at the next time step, given the safe input sequence of the current time step.

Now, the SMPC+FTP method is derived, consisting of two parts, SMPC and FTP, i.e., at every time step an SMPC OCP and an FTP OCP are solved. The general idea is that the first input $\mathbf{u}_{\text{SMPC},0}$ of the SMPC input sequence $\mathbf{U}_{\text{SMPC}} = [\mathbf{u}_{\text{SMPC},0}, \dots, \mathbf{u}_{\text{SMPC},N-1}]^\top$ must only be applied if, based on the first SMPC input $\mathbf{u}_{\text{SMPC},0}$, a fail-safe trajectory can be found as described below. Compared to regular SMPC methods, this approach guarantees that applying the optimistic SMPC input $\mathbf{u}_{\text{SMPC},0}$ does not lead to unsafe behavior. Therefore, at each time step one SMPC OCP and one FTP OCP is solved. The algorithm outline is shown in Figure 1.

1) *SMPC*: In the first part of SMPC+FTP an SMPC problem is solved on a finite horizon N_{SMPC} , yielding the input sequence $\mathbf{U}_{\text{SMPC}} = [\mathbf{u}_{\text{SMPC},0}, \dots, \mathbf{u}_{\text{SMPC},N_{\text{SMPC}}-1}]^\top$. This SMPC optimization takes into account the uncertain environment and constraints due to other traffic participants, i.e., target vehicles. Collision constraints are formulated as chance-constraints, based on a probabilistic TV prediction. Therefore, the planned SMPC trajectory provides an efficient and optimistic future trajectory for the EV, as it is not required to avoid collision with TVs for worst-case scenarios. However, chance-constraints allow a small probability of collision in the future, depending on the predefined SMPC risk parameter.

2) *FTP*: The second part of SMPC+FTP is based on FTP to ensure that the planned EV trajectory remains safe. First, a worst-case TV prediction is performed. Then, a fail-safe MPC problem on a finite horizon N_{FTP} is solved, resulting in an input sequence $\mathbf{U}_{\text{FTP}} = [\mathbf{u}_{\text{FTP},0}, \dots, \mathbf{u}_{\text{FTP},N_{\text{FTP}}-1}]^\top$. The fail-safe trajectory is required to avoid collision with the worst-case TV prediction and after applying the full fail-safe input sequence \mathbf{U}_{FTP} , the terminal state $\xi_{N_{\text{FTP}}}$ must be a safe state according to Definition 1.

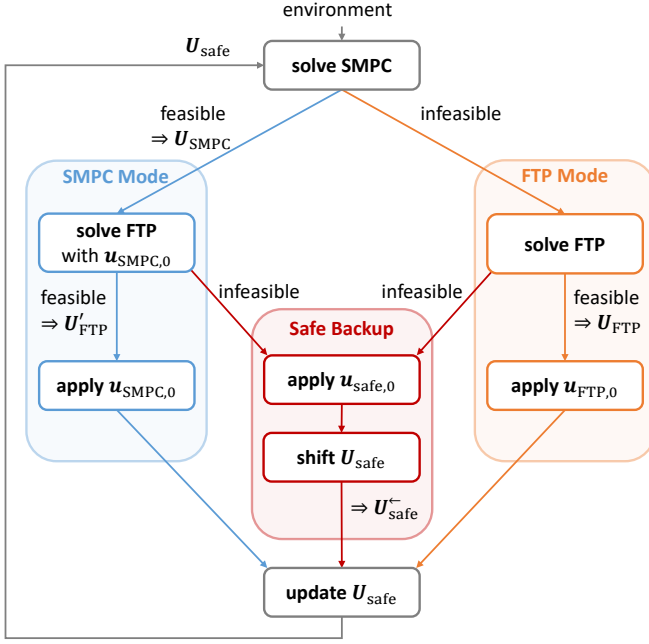


Fig. 1. SMPC+FTP procedure for each time step. Blue shows the ideal mode with an applied SMPC input, orange represents the safe alternative mode with an applied FTP input, and red indicates an infeasible FTP problem, which requires applying a safe backup input.

The exact FTP formulation depends on the feasibility of the SMPC OCP.

a) *Feasible SMPC*: If the SMPC OCP yields a solution, FTP is used to decide whether applying the first SMPC input $u_{SMPC,0}$ is safe. Therefore, an FTP OCP is formulated starting with the EV state obtained by applying the first SMPC input $u_{SMPC,0}$, i.e., the initial state for the FTP OCP is

$$\xi'_0 = f(\xi_0, u_{SMPC,0}) \quad (13)$$

with $f(\xi_0, u_{SMPC,0})$ according to (6).

If feasible, the FTP OCP yields a fail-safe input sequence U'_{FTP} , based on ξ'_0 . Therefore, the first element $u_{SMPC,0}$ of the SMPC input sequence is applied safely, as shown by the blue path in Figure 1. The resulting new safe input sequence is given by

$$U_{safe} = [U'_{FTP}, U_{brake}] \quad (14a)$$

$$U_{brake} = \left[\begin{bmatrix} a_{min} \\ 0 \end{bmatrix}, \begin{bmatrix} a_{min} \\ 0 \end{bmatrix}, \dots \right] \quad (14b)$$

where a_{min} is the maximal deceleration and U_{brake} is a braking sequence to bring the EV to a standstill. The safe input sequence U_{safe} ensures a safe state after the full fail-safe input sequence U'_{FTP} was applied and then initiates braking in order to reach zero velocity. Note that a_{min} is only applied in U_{brake} until a standstill is reached, subsequently no deceleration is applied.

b) *Infeasible SMPC*: If the SMPC OCP is infeasible, the FTP optimal control problem is solved with initial state ξ_0 for the FTP OCP. If an FTP solution U_{FTP} is found, the first element of U_{FTP} , i.e., $u_{FTP,0}$, is applied, as indicated by

the orange path in Figure 1. The updated safe input sequence follows from

$$U_{safe} = [U_{FTP,1:N_{FTP}}, U_{brake}] \quad (15)$$

with U_{brake} according to (14b) where

$$U_{FTP,1:N_{FTP}} = [u_{FTP,1}, \dots, u_{FTP,N_{FTP}-1}] \quad (16)$$

consists of all input elements of U_{FTP} except the first input $u_{FTP,0}$.

3) *Infeasible FTP*: In case of an infeasible FTP OCP no new input is generated at the current time step h . However, by definition the safe input sequence obtained at the previous time step $h-1$ remains safe for the current time step h . Therefore, in case that no solution exists to the FTP OCP, the first element of the still valid, safe input sequence U_{safe} is applied, which is denoted by $u_{safe,0}$. This procedure is highlighted in red in Figure 1.

Continuously applying the elements of U_{safe} results in a safe trajectory according to Definition 2. If the FTP OCP remains infeasible for consecutive time steps, multiple subsequent input elements of a single safe input sequence are potentially applied until the FTP OCP becomes feasible again.

This procedure requires shifting U_{safe} after each SMPC+FTP iteration where the FTP OCP was infeasible, i.e., the first input element $u_{safe,0}$ of U_{safe} was applied. The shifted updated input sequence is obtained by

$$U_{safe}^{\leftarrow} = U_{safe} \begin{bmatrix} 0_m \\ I_m \end{bmatrix} = [u_{safe,1}, u_{safe,2}, \dots, u_{safe,m}] \quad (17)$$

with $U_{safe} \in \mathbb{R}^{2 \times (m+1)}$, identity matrix $I_m \in \mathbb{R}^{m \times m}$, and $0_m \in \mathbb{R}^{1 \times m}$. The shifted safe input sequence U_{safe}^{\leftarrow} consists of all elements of U_{safe} except the already applied input $u_{safe,0}$.

Then, the safe input sequence is updated at the end of the SMPC+FTP iteration by selecting

$$U_{safe} = U_{safe}^{\leftarrow}, \quad (18)$$

which initializes the safe input sequence for the next SMPC+FTP iteration.

4) *Summary of SMPC+FTP*: Within the SMPC+FTP method four cases are considered. These cases are summarized in the following.

a) *SMPC and FTP feasible*: The first SMPC input $u_{SMPC,0}$ is applied and a new safe input sequence U_{safe} is obtained according to (14).

b) *SMPC infeasible and FTP feasible*: The first FTP input $u_{FTP,0}$ is applied and a new safe input sequence U_{safe} is obtained according to (15).

c) *SMPC feasible and FTP infeasible*: No new input sequence is obtained. The first input element of the safe input sequence $u_{safe,0}$ is applied. The safe input sequence U_{safe} remains valid for the next time step and is updated according to (18).

d) *SMPC infeasible and FTP infeasible*: As in the previous case, no new input sequence is obtained. The input $u_{safe,0}$ is applied and U_{safe} is generated based on (18) for the next time step.

In summary, the SMPC solution is applied as long as a fail-safe backup trajectory exists. Safety is guaranteed by solving

an FTP OCP, based on the first SMPC input. In cases where the FTP OCP is infeasible, the safe input sequence of the previous time step is still valid. Following this procedure, in regular cases the efficient SMPC inputs are applied, resulting in good performance, while FTP guarantees safety for all possible cases, including rare events.

B. Recursive Feasibility

A disadvantage of various SMPC algorithms is that recursive feasibility of the optimization problem cannot be guaranteed. In this section recursive feasibility of the SMPC+FTP method is proved, i.e., if the optimization problem can be solved at step h , it can also be solved at step $h + 1$ for all $h \in \mathbb{N}$. In this section it is necessary to denote the time step h . The safe input sequence updated at time step h is denoted by $U_{\text{safe},h}$.

Definition 3 (Safe Feasible Trajectory). *Let there exist a safe set Ξ_{safe} and let Ξ_f be a control invariant set. Let $\chi_h^U = [\xi_h, \dots, \xi_{h+N}]$ denote a trajectory starting at initial state ξ_h at time step h with N trajectory steps obtained by applying the input sequence $U_h = [u_h, \dots, u_{h+N-1}]$ with $\xi_{h+1} = f(\xi_h, u_h)$. Then, the set Γ_h of safe feasible trajectories, leading into the control invariant set Ξ_f , is defined as*

$$\Gamma_h = \left\{ \chi_h^U \mid \xi_{h+i} \in \Xi_{\text{safe}}, i \in \{0, \dots, N\}, \xi_{h+N} \in \Xi_f \right\}. \quad (19)$$

A safe feasible trajectory satisfies all constraints given by Ξ_{safe} and ends in the control invariant set Ξ_f .

Assumption 3 (System Models). *The ego vehicle system models (3) and (6) correspond to the dynamics of the real system. The target vehicle model (9) represents an over-approximation of the real target vehicle dynamics.*

Here, over-approximation means that the possible states reachable with the TV model include all possible states obtained with the real TV dynamics.

Assumption 4 (Initial Safe Input Sequence). *At the initial time step $h = 0$ the initial ego vehicle state is safe and there exists a known initial safe input sequence $U_{\text{safe},\text{init}}$, such that $\chi_0^{U_{\text{safe},\text{init}}}$ is a safe feasible trajectory, i.e., $\chi_0^{U_{\text{safe},\text{init}}} \in \Gamma_0$.*

We can now show recursive feasibility of the proposed method.

Theorem 1. *Let Assumptions 3 and 4 hold. Then for the SMPC+FTP approach there exists a feasible trajectory $\chi_h^U \in \Gamma_h$ that is guaranteed to be safe at all time steps $h \in \mathbb{N}$.*

Proof. The derivation of the proof is given in Appendix B. \square

Note that the worst-case behavior of the TVs depends on the traffic rules. Therefore, safety and recursive feasibility of the SMPC+FTP method can only be guaranteed if surrounding TVs adhere to the underlying traffic rules, as stated in Assumption 1. However, no specific traffic rules are required to prove Theorem 1.

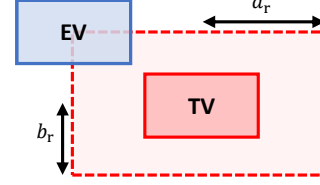


Fig. 2. Target vehicle safety rectangle.

V. TRAJECTORY PLANNING ALGORITHMS

The two MPC optimal control problems, SMPC and FTP, are solved independently. In the following, the respective optimal control problems are derived, specifically focusing on the safety constraints.

A. Stochastic Model Predictive Control

SMPC solves an optimal control problem with chance constraints, accounting for TV uncertainty, depending on a risk factor β . First, a safety area is defined around each predicted TV state which accounts for the EV and TV shape. Then, this safety area is increased to account for TV uncertainty, given a predefined risk parameter. Eventually, a linear constraint is generated for each TV, depending on the positioning of the EV and the TV.

1) *Deterministic Target Vehicle Prediction:* For SMPC a simple TV prediction is applied, representing the most likely TV behavior with $w_k^{\text{TV}} = \mathbf{0}$, i.e., $u_k^{\text{TV}} = \tilde{u}_k^{\text{TV}}$. It is assumed that the current TV maneuver continues for the prediction horizon N_{SMPC} . Therefore, TV model (9) is applied where the TV reference $\xi_{\text{ref},k}^{\text{TV}}$ depends on the current TV maneuver. The reference velocity $v_{x,\text{ref},k}^{\text{TV}}$ is set to the current TV velocity $v_{x,0}^{\text{TV}}$. The TV reference lateral velocity is chosen to be $v_{y,\text{ref},k}^{\text{TV}} = 0$. The reference lateral position $y_{\text{ref},k}^{\text{TV}}$ is the current TV lane center. A new reference lane is selected if part of the TV shape lies in this adjacent lane and the lateral velocity moves the TV towards this adjacent lane. If both of these requirements are fulfilled, the adjacent lane center is selected as the lateral position reference.

2) *Target Vehicle Safety Area:* Collisions with TVs are avoided by ensuring the necessary distance between the EV and TV. Here, a safety rectangle around the TV is defined. While it is possible to choose other shapes, e.g., ellipses as in [38], rectangles allow to easily generate linear constraints, as described in Section V-A4.

The safety rectangle with length a_r and width b_r is illustrated in Figure 2. In order to ensure that the vehicle shapes do not intersect, the vehicle centers need to be distanced at least by the vehicle length l_{veh} and width w_{veh} . For the safety rectangle width this yields

$$b_r = w_{\text{veh}} + \varepsilon_{\text{safe}} \quad (20)$$

where $\varepsilon_{\text{safe}}$ is a possible additional safety margin.

Calculating the safety rectangle length a_r requires a velocity dependent part $\tilde{a}_r(\xi, \xi^{\text{TV}})$, compensating for a potential velocity difference between the EV and the TV, resulting in

$$a_r = l_{\text{veh}} + \varepsilon_{\text{safe}} + \tilde{a}_r(\xi, \xi^{\text{TV}}). \quad (21)$$

The velocity dependent part \tilde{a}_r needs to account for the difference in traveled distance between the EV and TV if both vehicles initiate maximal braking, e.g., in an emergency braking scenario. Here, in addition to Assumption 2, zero reaction time is assumed. The traveled distance Δx of a vehicle until standstill is described by

$$\begin{aligned}\Delta x(t_{\text{stop}}) &= v_x t_{\text{stop}} + 0.5 a_{\min}(t_{\text{stop}})^2 \\ &= -\frac{1}{a_{\min}}(v_x)^2\end{aligned}\quad (22a)$$

$$t_{\text{stop}} = -\frac{v_x}{a_{\min}} \quad (22b)$$

with maximal longitudinal deceleration a_{\min} , time to standstill t_{stop} , given the initial EV and TV velocity v and v_x^{TV} , respectively. Based on the difference in traveled distance

$$\Delta x^{\text{EV}}(t_{\text{stop}}^{\text{EV}}) - \Delta x^{\text{TV}}(t_{\text{stop}}^{\text{TV}}) = -\frac{1}{a_{\min}}(v^2 - (v_x^{\text{TV}})^2), \quad (23)$$

assuming similar maximal deceleration for the EV and TV, the velocity dependent safety distance is obtained by

$$\tilde{a}_r(\xi, \xi^{\text{TV}}) = -\frac{1}{a_{\min}} \max\left\{0, \left(v^2 - (v_x^{\text{TV}})^2\right)\right\} \quad (24)$$

where the max-operator ensures that the safety rectangle length does not decrease for $v_x^{\text{TV}} > v$.

For the SMPC optimal control problem the safety rectangle length and width is calculated for prediction time step k , based on the TV prediction ξ_k^{TV} described in Section V-A1. However, only the initial EV state ξ_0 is considered in the velocity depended part \tilde{a}_r . This is necessary in order to generate linear safety constraints. While it would be possible to use predicted EV states, these would yield nonlinear constraints. The resulting safety rectangle parameters are

$$b_{r,k} = w_{\text{veh}} + \varepsilon_{\text{safe}} \quad (25a)$$

$$a_{r,k} = l_{\text{veh}} + \varepsilon_{\text{safe}} + \tilde{a}_r(\xi_0, \xi_k^{\text{TV}}). \quad (25b)$$

3) *Chance Constraint Reformulation:* The TV safety rectangle given by (25) only considers the deterministic prediction, but it does not account for TV uncertainty. In the following the safety rectangle is enlarged, based on a chance constraint depending on the TV uncertainty and a predefined risk parameter β . The chance constraint, similar to (1e), is given by

$$\Pr(\xi_k \in \Xi'_{k,\text{safe}}(w_k^{\text{TV}})) \geq \beta \quad (26)$$

where the safe set $\Xi'_{k,\text{safe}}(w_k^{\text{TV}})$ for the EV state depends on the previously defined safety rectangle parameters of (25) and the TV uncertainty w_k^{TV} . In other words, the previously defined safety area is now enlarged to account for TV uncertainty. A large risk parameter reduces risk by generating a large safety area around the TV.

The chance constraint (26) cannot be solved directly. In the following, a deterministic approximation is determined for this probabilistic expression, inspired by other SMPC approaches [9], [38].

According to (9) the TV state follows

$$\xi_{k+1}^{\text{TV}} = A\xi_k^{\text{TV}} + BK(\xi_k^{\text{TV}} - \xi_{\text{ref},k}^{\text{TV}}) + Bw_k^{\text{TV}}, \quad (27)$$

while the predicted TV state is given by

$$\hat{\xi}_{k+1}^{\text{TV}} = A\hat{\xi}_k^{\text{TV}} + BK(\hat{\xi}_k^{\text{TV}} - \xi_{\text{ref},k}^{\text{TV}}), \quad (28)$$

yielding the prediction error

$$e_k = \hat{\xi}_k^{\text{TV}} - \xi_k^{\text{TV}}. \quad (29)$$

The TV prediction (28) is now split into a deterministic and a stochastic part

$$\hat{\xi}_{k+1}^{\text{TV}} = \xi_{k+1}^{\text{TV}} + (A + BK)e_k - Bw_k^{\text{TV}} = \xi_{k+1}^{\text{TV}} + e_{k+1} \quad (30)$$

which results in the prediction error update

$$e_{k+1} = (A + BK)e_k - Bw_k^{\text{TV}}. \quad (31)$$

Given the sensor noise w_0^{sens} according to (12), the initial error follows $e_0 \sim \mathcal{N}(0, \Sigma_0^e)$ with $\Sigma_0^e = \Sigma_0^{\text{sens}}$. As both the TV uncertainty, with covariance matrix Σ_w^{TV} , and the sensor noise are assumed to be Gaussian distributions, a recursive computation of the prediction error covariance matrix Σ_k^e is possible, yielding

$$\Sigma_{k+1}^e = B\Sigma_w^{\text{TV}}B^\top + (A + BK)\Sigma_k^e(A + BK)^\top. \quad (32)$$

Based on the prediction error covariance matrix Σ_k^e , the TV safety rectangle is increased. Given a predefined SMPC risk parameter β , the aim is to find a region around the predicted TV state which contains the true TV state with probability β . This then allows to consider the probabilistic safety constraint (26) as a deterministic substitute constraint. As the TV safety rectangle only considers positions, we define the reduced error $\tilde{e}_k = [e_{x,k}, e_{y,k}]^\top$ with the reduced covariance matrix

$$\tilde{\Sigma}_k^e = \begin{bmatrix} \sigma_{x,k}^2 & 0 \\ 0 & \sigma_{y,k}^2 \end{bmatrix} \quad (33)$$

with variances $\sigma_{x,k}^2$ and $\sigma_{y,k}^2$ for the longitudinal and lateral TV position, corresponding to the first and third diagonal element of Σ_k^e .

Lemma 1. *The reduced error covariance matrix $\tilde{\Sigma}_k^e$ corresponding to the position coordinates is obtained from Σ_k^e by omitting the correlation to the respective velocities.*

Proof. The proof is given in Appendix C. \square

The reduced error covariance matrix $\tilde{\Sigma}_k^e$ is now used to enlarge the safety rectangle to account for uncertainty. Note that the error covariance matrix Σ_k^e is still required to compute (32).

The bivariate Gaussian distribution described by $\tilde{\Sigma}_k^e$ with mean $\mu = [\mu_x, \mu_y]^\top = \mathbf{0}$ consists of independent random variables for longitudinal and lateral position. This allows to find a confidence region around the predicted TV state mean, bounded by an ellipsoidal isoline enclosing the highest density region as illustrated in Figure 3. The aim is to find an isoline which contains the prediction error with a probability according to risk parameter β . The isoline ellipse equation is denoted by

$$(\tilde{e}_k - \mu)^\top (\tilde{\Sigma}_k^e)^{-1} (\tilde{e}_k - \mu) = \kappa \quad (34a)$$

$$\frac{(e_{x,k} - \mu_x)^2}{\sigma_{x,k}^2} + \frac{(e_{y,k} - \mu_y)^2}{\sigma_{y,k}^2} = \kappa \quad (34b)$$

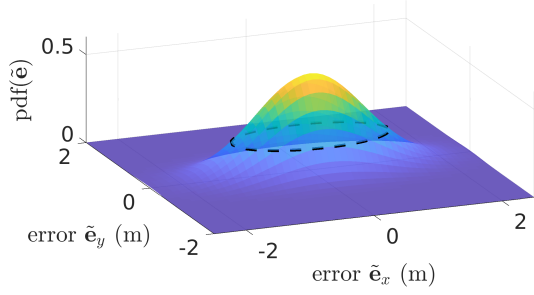


Fig. 3. Exemplary bivariate Gaussian probability distribution function of the prediction error $\tilde{\mathbf{e}}$, including an isoline (dotted black line).

with tolerance level κ . The tolerance level κ is determined based on the *chi-squared distribution* $\chi_n^2(1 - \beta)$, given the risk parameter β and the number of degrees of freedom n . In this case, $n = 2$ as the reduced error $\tilde{\mathbf{e}}_k$ consists of two elements. It then follows that

$$\kappa = \chi_2^2(1 - \beta), \quad (35)$$

which ensures that the probability of the true TV state not lying within the isoline is $100(1 - \beta)\%$, where the isoline is defined by the tolerance level κ . The ellipse semi-major and semi-minor axes are then given by

$$e_{x,k,\kappa} = \sigma_{x,k} \sqrt{\kappa} \quad (36a)$$

$$e_{y,k,\kappa} = \sigma_{y,k} \sqrt{\kappa}. \quad (36b)$$

These ellipse parameters are now used to increase the TV safety rectangle.

Remark 1. *Instead of using the chi-squared distribution, in this case the tolerance level can also be obtained by $\kappa = -2 \ln \beta$.*

While an ellipse, according to (34), describes the desired confidence region, the constraint generation method used in this work requires a rectangular TV safety area. We therefore over-approximate the ellipse by a rectangle. In order to include this uncertainty consideration in the rectangle parameters $a_{r,k}$ and $b_{r,k}$ of (25), the rectangle parameters are increased based on the ellipse semi-major axis $e_{x,k,\kappa}$ and semi-minor axis $e_{y,k,\kappa}$, resulting in

$$b_{r,k} = w_{\text{veh}} + \varepsilon_{\text{safe}} + e_{y,k,\kappa} \quad (37a)$$

$$a_{r,k} = l_{\text{veh}} + \varepsilon_{\text{safe}} + \tilde{a}_r(\xi_0, \xi_k^{\text{TV}}) + e_{x,k,\kappa}. \quad (37b)$$

The updated safety rectangle parameters are now utilized to generate the safety constraints for the SMPC optimal control problem.

4) *SMPC Constraint Generation:* Given the safety rectangles for each TV, linear constraints to avoid collisions can be defined for each prediction step and for each TV. Each linear constraint is of the form

$$0 \geq q_y(\xi_0, \xi_k^{\text{TV}}) d_k + q_x(\xi_0, \xi_k^{\text{TV}}) s_k + q_t(\xi_0, \xi_k^{\text{TV}}) \quad (38)$$

where q_y and q_x are the coefficients for the EV states d_k and s_k , respectively, and q_t is the intercept. The coefficients q_y , q_x , and q_t of the linear constraint depend on the current

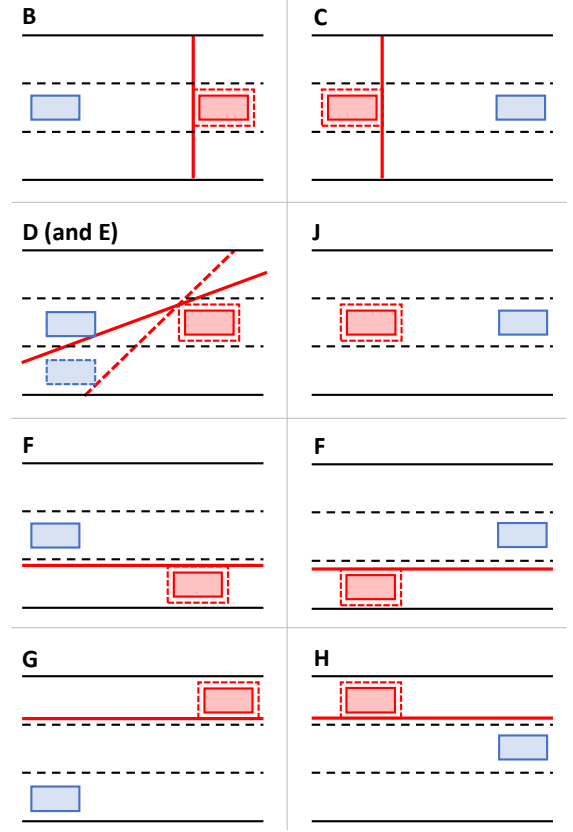


Fig. 4. Selected constraint generation cases for SMPC. Driving direction is from left to right. The EV and TV are shown in blue and red, respectively. The dashed red line represents the safety area around the TV.

EV state ξ_0 and the predicted mean TV states ξ_k^{TV} . This results in multiple constraint generation cases, where the major cases are displayed in Figure 4. The cases are distinguished based on the initial vehicle configuration at the beginning of the optimal control problem, i.e., $k = 0$. As mentioned in Section V-A2, while the predicted TV state ξ_k^{TV} at prediction step k is considered to build the constraint given a specific case, only the initial EV state ξ_0 is considered in order to allow generating linear constraints. We now introduce a brief, but not necessarily complete overview of constraint cases that are considered, which is an extension to the cases in [10]. A complete overview of cases, requirements, and constraint parameters q_x , q_y , q_t from (38) is found in Appendix D.

We first consider the case where the TV is far away from the EV, i.e., a longitudinal distance $\Delta x_0^{\text{EV,TV}} = s_0 - x_0^{\text{TV}}$ which is larger than r_{lar} . Therefore, no constraint is generated.

A) $|\Delta x_0^{\text{EV,TV}}| \geq r_{\text{lar}}$: no constraint

Then, the remaining cases are addressed with a longitudinal distance $|\Delta x_0^{\text{EV,TV}}| < r_{\text{lar}}$. Further cases are distinguished given how close the TV is positioned to the EV, based on a function f_{close} , which is further explained in Appendix D. For simplicity, f_{close} is assumed to be a constant r_{close} here. In case of a vehicle distance $|\Delta x_0^{\text{EV,TV}}| > r_{\text{close}}$, a vertical constraint is used behind the TV (case B) or in front of the TV (case C).

B) $-(\Delta x_0^{\text{EV,TV}}) > r_{\text{close}}$: vertical constraint behind TV

C) $(\Delta x_0^{\text{EV,TV}}) > r_{\text{close}}$: vertical constraint in front of TV

If the EV is located closely behind the TV, i.e., $s_0 < x_0^{\text{TV}}$ and $-(\Delta x_0^{\text{EV,TV}}) \leq r_{\text{close}}$, the constraint depends on the respective current EV and TV lanes $y_{\text{lane},0}^{\text{EV}}$ and $y_{\text{lane},0}^{\text{TV}}$. In general, the plan is to overtake TVs on the left side. If the vehicles are in the same lane (case D), an inclined constraint is applied allowing the EV to switch to a lane left of the TV. The constraint slope is bounded to a horizontal or vertical line. If a TV is on an adjacent lane to the left of the EV, i.e., $y_{\text{lane},0}^{\text{EV}} + w_{\text{lane}} = y_{\text{lane},0}^{\text{TV}}$ with lane width w_{lane} , an inclined (bounded) constraint is also applied (case E).

D) $y_{\text{lane},0}^{\text{EV}} = y_{\text{lane},0}^{\text{TV}}, -(\Delta x_0^{\text{EV,TV}}) \leq r_{\text{close}}$: inclined constraint connecting EV and TV

E) $y_{\text{lane},0}^{\text{EV}} + w_{\text{lane}} = y_{\text{lane},0}^{\text{TV}}, (x_0^{\text{TV}} - s_0) \leq r_{\text{close}}$: inclined constraint connecting EV and TV

If the TV is on a lane to the right of the EV, i.e., $y_{\text{lane},0}^{\text{EV}} > y_{\text{lane},0}^{\text{TV}}$ (case F), a horizontal constraint is employed at the TV safety rectangle. If the TV is in front of the TV and at least two lanes to the left of the EV, i.e., $y_{\text{lane},0}^{\text{EV}} + 2w_{\text{lane}} \leq y_{\text{lane},0}^{\text{TV}}$ (case G), or behind the EV and at least one lane to the left of the TV (case H), i.e., $y_{\text{lane},0}^{\text{EV}} + w_{\text{lane}} \leq y_{\text{lane},0}^{\text{TV}}$, again a horizontal constraint is employed.

F) $y_{\text{lane},0}^{\text{EV}} > y_{\text{lane},0}^{\text{TV}}, |\Delta x_0^{\text{EV,TV}}| \leq r_{\text{close}}$: horizontal constraint left of the TV

G) $y_{\text{lane},0}^{\text{EV}} + 2w_{\text{lane}} \leq y_{\text{lane},0}^{\text{TV}}, -(\Delta x_0^{\text{EV,TV}}) \leq r_{\text{close}}$: horizontal constraint right of the TV

H) $y_{\text{lane},0}^{\text{EV}} + w_{\text{lane}} \leq y_{\text{lane},0}^{\text{TV}}, (\Delta x_0^{\text{EV,TV}}) \leq r_{\text{close}}$: horizontal constraint right of the TV

Finally, if the EV is positioned in front of the TV on the same lane, it is assumed that the TV keeps its distance to the EV. Therefore, no constraint is generated (case J).

J) $y_{\text{lane},0}^{\text{EV}} = y_{\text{lane},0}^{\text{TV}}, (\Delta x_0^{\text{EV,TV}}) \leq r_{\text{close}}$: no constraint

The presented cases are now used to formulate safety constraints in the SMPC OCP.

5) *SMPC Optimal Control Problem*: With the definition of the safety constraints, the deterministic optimal control problem replacing the SMPC problem is given by

$$V^* = \min_U \sum_{k=1}^{N_{\text{SMPC}}} \|\Delta \xi_k\|_Q + \|u_{k-1}\|_R + \|\Delta u_{k-1}\|_S \quad (39a)$$

$$\text{s.t. } \xi_{k+1} = f^d(\xi_0, \xi_k, u_k) \quad (39b)$$

$$\xi_{k+1}^{\text{TV}} = A\xi_k^{\text{TV}} + B\tilde{u}_k^{\text{TV}} \quad (39c)$$

$$\xi_k \in \Xi \quad \forall k \in \{1, \dots, N_{\text{SMPC}}\}, \quad (39d)$$

$$u_k \in \mathcal{U} \quad \forall k \in \{0, \dots, N_{\text{SMPC}} - 1\}, \quad (39e)$$

$$0 \geq q_y(\xi_0, \xi_k^{\text{TV}})d_k + q_x(\xi_0, \xi_k^{\text{TV}})s_k + q_t(\xi_0, \xi_k^{\text{TV}}) \quad (39f)$$

$$\forall k \in \{0, \dots, N_{\text{SMPC}}\}$$

where $\Delta \xi_k = \xi_k - \xi_{k,\text{ref}}$ with EV reference state $\xi_{k,\text{ref}}$ and the linear function f^d according to (6). For the input difference Δu , u_{-1} is set to the applied input of the previous time step. The cost function sum limits are shifted to include a terminal cost for ξ_N . The weighting matrices are given by Q , S , and R . We consider constant input constraints \mathcal{U} according to (7) and state constraints Ξ according to (8).

The resulting SMPC optimal control problem (39) is a quadratic program with linear constraints, accounting for uncertainty with the chance constraint reformulation described in Section V-A3. This optimal control problem can be solved efficiently, where the major calculation steps to obtain the linear constraints (39f) are performed before the optimization starts.

B. Failsafe Trajectory Planning

While the SMPC algorithm only accounts for part of the TV uncertainty in order to plan an optimistic trajectory, the backup FTP algorithm needs to consider worst-case uncertainty realizations. This is achieved based on reachability analysis. First, the worst-case TV occupancy prediction is determined. Then, linear constraints are generated based on the TV predictions. Eventually, given a safe invariant terminal set, the FTP optimal control problem is solved.

1) *Target Vehicle Occupancy Prediction*: Similar to the SMPC algorithm, a rectangular safety area surrounding each TV is defined. However, for the FTP the maximal reachable area needs to be determined. First, it is necessary to define certain traffic rules to which the TV adheres, according to Assumption 1:

- Road boundaries apply.
- Negative velocities are forbidden.
- Collisions with vehicles directly in front of the TV (in the same lane) must be avoided.
- Only a single lane change is allowed (within the prediction horizon).
- No lane change is allowed if the TV velocity is below a predefined minimal lane change velocity $v_{\text{LC,min}}$.
- No lane change is allowed if the distance to a vehicle on the new lane becomes too small.

As linear dynamics are assumed for the TV motion, the minimal and maximal possible TV inputs are used to determine the maximal reachable set, inspired by [11], [25], [28].

The set of all possible locations reachable for a TV at prediction step k is denoted by the reachable set $\mathcal{R}_k^{\text{TV}}$, including the TV and shape. While referring to $\mathcal{R}_k^{\text{TV}}$ as the reachable set of the TV, we additionally enlarge this set accounting for the EV shape. This is necessary as the set $\mathcal{R}_k^{\text{TV}}$ is later used to avoid collisions by keeping the EV center outside of $\mathcal{R}_k^{\text{TV}}$. Given the solution $\zeta(\hat{\xi}_0^{\text{TV}}, U)$ to the TV dynamics (9) starting at the initial state $\hat{\xi}_0^{\text{TV}}$ applying an input sequence U , we define the reachable set

$$\mathcal{R}_k^{\text{TV}} = \left\{ \zeta(\hat{\xi}_0^{\text{TV}}, U) \mid U(i) \in \mathcal{U}^{\text{TV}} \quad \forall i \in \{0, \dots, k-1\}, \quad \hat{\xi}_0^{\text{TV}} \in \Xi_0^{\text{TV}} \right\}. \quad (40)$$

The initial state for the reachable set $\mathcal{R}_k^{\text{TV}}$ is not the TV state ξ_0^{TV} , but depends on the sensor uncertainty as well as the TV and EV shape. This initial set is given by

$$\Xi_0^{\text{TV}} = \left\{ \hat{\xi}_0^{\text{TV}} \mid \hat{\xi}_0^{\text{TV}} + \min\{w_0^{\text{sens}}\} - [l_{\text{veh}}, 0, w_{\text{veh}}, 0]^T \leq \hat{\xi}_0^{\text{TV}}, \right. \\ \left. \hat{\xi}_0^{\text{TV}} \leq \hat{\xi}_0^{\text{TV}} + \max\{w_0^{\text{sens}}\} + [l_{\text{veh}}, 0, w_{\text{veh}}, 0]^T \right\}. \quad (41)$$

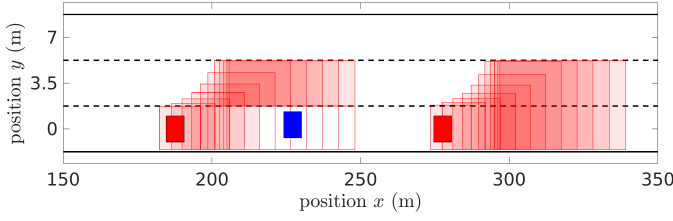


Fig. 5. Target vehicle occupancy sets for multiple prediction steps with the EV in blue and TVs in red. Areas shaded in red depict areas possibly occupied by a TV. As the TVs must avoid collision with vehicles in front, the left TV cannot occupy the area in the EV lane close to the EV. A TV double lane change is not considered.

The initial set Ξ_0^{TV} in (41) can be interpreted as a rectangle defined by two corners. As we assume a linear TV prediction model, the reachable set $\mathcal{R}_k^{\text{TV}}$ is calculated for prediction steps $k > 0$ by applying the maximal and minimal inputs $\mathbf{u}^{\text{TV}} \in \mathcal{U}^{\text{TV}}$, while adhering to traffic rules.

The reachable set is only calculated at discrete time steps. In order to account for a continuous system, the final reachable set $\bar{\mathcal{R}}_k^{\text{TV}}$ is obtained by building a rectangular convex hull, covering two consecutive prediction steps, i.e.,

$$\bar{\mathcal{R}}_k^{\text{TV}} = \text{conv} \{ \mathcal{R}_{k-1}^{\text{TV}}, \mathcal{R}_k^{\text{TV}} \} \quad (42)$$

where conv denotes the convex hull operation.

A special case is considered if the TV is located behind the EV in the same lane. The TV must not collide with the EV in the same lane, however, the TV is allowed to switch lanes in order to pass the EV. Here, this is accounted for by treating this special case in the following way. Three placeholder TV reachable sets describe the possible TV behavior. The first placeholder TV reachable set is based in the EV lane such that collisions with the EV are avoided. The other two placeholder TV reachable sets cover the admissible adjacent lanes left and right of the EV, representing the reachable sets for a potential TV lane change. Figure 5 shows an example of areas possibly occupied by TVs for multiple prediction steps.

2) *FTP Constraint Generation*: Once the reachable sets $\bar{\mathcal{R}}_k^{\text{TV}}$ for each TV are determined, linear constraints are generated. We again consider different cases regarding varying EV and TV positions. The cases are similar to those of Section V-A4, with a few variations. FTP cases are denoted with an asterisk. Same letters indicate similar SMPC and FTP case types. The major FTP cases are illustrated in Figure 6. Again, a complete overview of the FTP cases, requirements, and constraint parameters q_x, q_y, q_t is found in Appendix D.

As for SMPC, we initially consider the case where the TV is farther away from the EV and therefore no constraint is generated (case A*).

A*) $|\Delta x_0^{\text{EV,TV}}| \geq r_{\text{lar}}$: no constraint

Then, all remaining cases are considered with a distance $|\Delta x_0^{\text{EV,TV}}| < r_{\text{lar}}$. First, cases are addressed where the EV is behind the TV (case B*) with a distance $-(\Delta x_0^{\text{EV,TV}}) > r_{\text{close}}^{\text{FTP}}$, which leads to a vertical constraint behind the TV. In contrast to case D of SMPC, in FTP overtaking is not actively planned. Therefore, if the EV is in the same lane behind the TV, a vertical constraint is employed (case D*), similar to case B*.

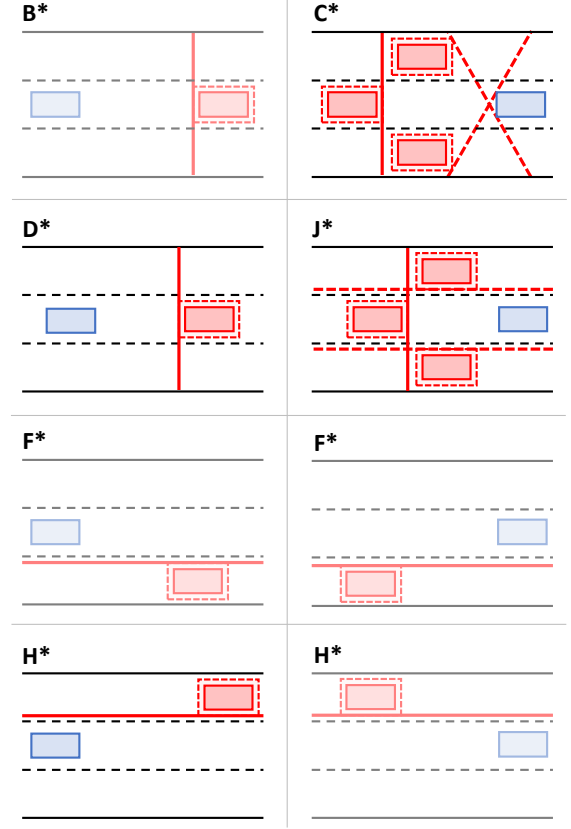


Fig. 6. Selected constraint generation cases for FTP. Cases equal to SMPC constraint generation cases have lighter colors. Driving direction is from left to right. The EV and TV are shown in blue and red, respectively. The dashed red line represents the safety area around the TV.

B*) $-(\Delta x_0^{\text{EV,TV}}) > r_{\text{close}}^{\text{FTP}}$: vertical constraint behind TV
D*) $y_{\text{lane},0}^{\text{EV}} = y_{\text{lane},0}^{\text{TV}}, -(\Delta x_0^{\text{EV,TV}}) \leq r_{\text{close}}^{\text{FTP}}$: vertical constraint behind TV

We now consider further cases where the EV and TV are close to each other, i.e., $|\Delta x_0^{\text{EV,TV}}| \leq r_{\text{close}}^{\text{FTP}}$. In case the EV is located on a different lane than the TV, horizontal constraints are generated at the TV, independent of the relative longitudinal positioning (cases F* and H*).

F*) $y_{\text{lane},0}^{\text{EV}} > y_{\text{lane},0}^{\text{TV}}, |\Delta x_0^{\text{EV,TV}}| \leq r_{\text{close}}^{\text{FTP}}$: horizontal constraint left of the TV
H*) $y_{\text{lane},0}^{\text{EV}} < y_{\text{lane},0}^{\text{TV}}, |\Delta x_0^{\text{EV,TV}}| \leq r_{\text{close}}^{\text{FTP}}$: horizontal constraint right of the TV

The last cases required focuses on the EV located in front of the TV in the same lane. In SMPC, no constraint was generated (case J). However, even though the TV is required to avoid collisions with another vehicle in front, for safety reasons we account for TVs located behind the EV in FTP. As stated in Section V-B1, in these cases up to three placeholder TV predictions are made, accounting for possible lane changes and overtaking maneuvers by the TV. If the distance between the EV and TV is smaller, i.e., $(\Delta x_0^{\text{EV,TV}}) \leq r_{\text{close}}^{\text{FTP}}$, a vertical constraint is employed for the TV prediction in the EV lane, while horizontal constraints are formed for TV predictions in adjacent lanes (case J*). If the distance is larger, i.e.,

$(\Delta x_0^{\text{EV,TV}}) > r_{\text{close}}^{\text{FTP}}$, inclined constraints are generated for TV predictions in lanes next to the EV, allowing more EV movement (case C*).

J*) $y_{\text{lane},0}^{\text{EV}} = y_{\text{lane},0}^{\text{TV}}$, $(\Delta x_0^{\text{EV,TV}}) \leq r_{\text{close}}^{\text{FTP}}$: (maximum of) three TV predictions with vertical and horizontal constraints

C*) $y_{\text{lane},0}^{\text{EV}} = y_{\text{lane},0}^{\text{TV}}$, $(\Delta x_0^{\text{EV,TV}}) > r_{\text{close}}^{\text{FTP}}$: (maximum of) three TV predictions with vertical and inclined constraints

Overall, the constraints generated for FTP are more conservative than for SMPC. This is due to the FTP aim of finding a trajectory which ends in a safe state. This would be complicated by incentivizing FTP to plan overtaking maneuvers. Details on finding a safe terminal state for the FTP optimal control problem are given in the following.

3) *Safe Invariant Terminal Set*: In addition to the regular safety constraints, a safe invariant terminal set is required to ensure safe EV inputs after the finite MPC prediction horizon. If, repeatedly, no solution to the SMPC and FTP optimal control problems is found, all safe backup inputs will be eventually applied. The FTP inputs are designed in such a way that they remain safe over the prediction horizon. However, after N_{FTP} inputs are applied and no new FTP solution is obtained, an emergency strategy has to be applied to come to a standstill. This is achieved by braking, while maintaining a constant steering angle $\delta = 0$, according to (14) and (15). Therefore, the terminal state of the FTP optimal control problem needs to fulfill certain requirements. First, the vehicle orientation must be aligned with the road, i.e., $\phi = 0$. This guarantees that braking and a constant steering angle $\delta = 0$ keep the EV within its current lane. Second, the distance to a TV in front of the EV must be large enough that no collision occurs if both vehicles initiate maximal deceleration. This is accounted for by

$$s_N \leq x_N^{\text{TV}} - \Delta s_{N_{\text{FTP}},\min} \quad (43a)$$

$$v_N \leq v_{N_{\text{FTP}},\max} \quad (43b)$$

with minimal terminal safety distance $\Delta s_{N_{\text{FTP}},\min}$ and maximal terminal safety velocity

$$v_{N_{\text{FTP}},\max} = v_{N_{\text{FTP}},\min}^{\text{TV}} - \sqrt{2\Delta s_{N_{\text{FTP}},\min} a_{x,\min}} \quad (44)$$

where $v_{N_{\text{FTP}},\min}^{\text{TV}}$ is the lowest predicted longitudinal TV velocity. Both (43) and (44) combined ensure that the minimal terminal safety distance $\Delta s_{N_{\text{FTP}},\min}$ is large enough such that, given a maximal EV velocity $v_{N_{\text{FTP}},\max}$, maximal deceleration of the EV guarantees collision avoidance for $k > N_{\text{FTP}}$. This less intuitive terminal constraint again has the advantage of yielding linear constraints.

4) *FTP Optimal Control Problem*: An optimal control problem with a similar structure compared to (39) is applied

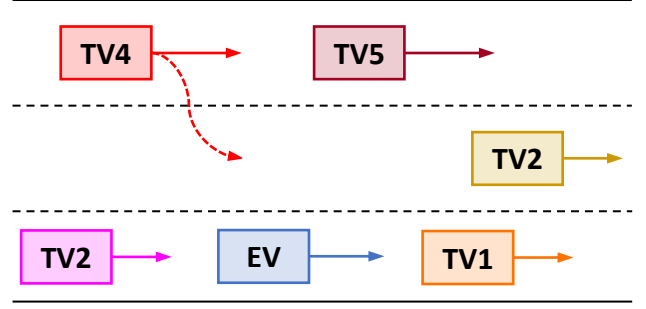


Fig. 7. Setup for both investigated scenarios (regular and emergency scenario).

for the FTP, yielding

$$V^* = \min_U \sum_{k=1}^{N_{\text{FTP}}} \|\Delta \xi_k\|_Q + \|u_{k-1}\|_R + \|\Delta u_{k-1}\|_S \quad (45a)$$

$$\text{s.t. } \xi_{k+1} = f^d(\xi_0, \xi_k, u_k) \quad (45b)$$

$$\xi_k \in \Xi \quad \forall k \in \{1, \dots, N_{\text{FTP}}\}, \quad (45c)$$

$$u_k \in \mathcal{U} \quad \forall k \in \{0, \dots, N_{\text{FTP}} - 1\}, \quad (45d)$$

$$0 \geq q_y \left(\xi_0, \bar{\mathcal{R}}_k^{\text{TV}} \right) d_k + q_x \left(\xi_0, \bar{\mathcal{R}}_k^{\text{TV}} \right) s_k + q_t \left(\xi_0, \bar{\mathcal{R}}_k^{\text{TV}} \right) \quad \forall k \in \{0, \dots, N_{\text{FTP}}\} \quad (45e)$$

$$s_N \leq x_N^{\text{TV}} - \Delta s_{N_{\text{FTP}},\min} \quad (45f)$$

$$v_N \leq v_{N_{\text{FTP}},\max} \quad (45g)$$

with the linear function f^d according to (6). The probabilistic constraint (39f) is now changed to constraint (45e), accounting for the worst-case TV uncertainty realizations. Similar to the SMPC optimal control problem, (45) is a quadratic program with linear constraints, which can be solved efficiently.

VI. RESULTS

We evaluate the proposed SMPC+FTP algorithm in different settings. In the following, the simulation setup is introduced first. Then, SMPC+FTP is analyzed and compared to an SMPC approach and an FTP approach in two scenarios.

A. Simulation Setup

In this simulation section we analyze the scenario illustrated in Figure 7. The EV is located on the right lane on a three-lane highway. We consider five TVs surrounding the EV on the highway. The goal for the EV is to safely and efficiently maneuver through traffic. The specific aims are to avoid collisions while maintaining a velocity close to a chosen reference velocity.

Given the initial scenario setup, we consider two different scenarios:

- 1) Regular scenario: All TVs keep their initial velocities and lanes.
- 2) Emergency scenario: One of the TVs (TV5) performs an emergency braking maneuver. This causes TV4 to avoid TV5 by moving to the center lane. This is followed by

a soft braking maneuver of TV1 to account for possible hazards. Eventually, TV4 moves to the left lane again to pass TV2.

The first scenario represents a regular scenario with no unexpected TV behavior. The second scenario covers a rare case, where a series of unexpected TV actions results in a challenging situation for the autonomous EV.

The simulations are carried out in Matlab using the *fmincon* solver on a desktop computer with an AMD Ryzen 7 1700X processor. The algorithms are based on the NMPC toolbox [43]. In the following, setup parameters are introduced which remain constant throughout the different simulations. All quantities are given in SI units. Units are omitted if clear by context.

The road consists of three lanes with lane width $w_{\text{lane}} = 3.5$ m. All vehicles have the same rectangular shape with length $l_{\text{veh}} = 5$ m and width $w_{\text{veh}} = 2$ m.

All MPC algorithms use a sampling time $T = 0.2$ s. The MPC optimization horizon is chosen to be the same for each MPC algorithm, i.e., the SMPC horizon is $N_{\text{SMPC}} = 10$ and the FTP horizon is $N_{\text{FTP}} = 10$. The linearized, time-discrete EV prediction model and constraints follow (6)-(8) with $l_f = l_r = 2$. The TV prediction model is given by (9)-(11a). The maximum and minimum acceleration and steering angle for the EV are $\mathbf{u}_{\text{max}} = [5, 0.2]^\top$, $\mathbf{u}_{\text{min}} = [-9, -0.2]^\top$, respectively. For the TV with a point-mass prediction model the maximal and minimal accelerations in x - and y -direction are $\mathbf{u}_{\text{max}}^{\text{TV}} = [5, 0.4]^\top$, $\mathbf{u}_{\text{min}}^{\text{TV}} = [-9, -0.4]^\top$. The EV input rate constraints are $-\Delta \mathbf{u}_{\text{min}} = \Delta \mathbf{u}_{\text{max}} = [9, 0.4]^\top$. The lane boundaries follow from the lane width and vehicle width, i.e., the vehicle shape must remain within the road. The maximal velocity is $v_{\text{max}} = 35 \text{ m s}^{-1}$. The elements of the assumed TV feedback controller matrix \mathbf{K} of (11a) are $k_{12} = -0.55$, $k_{21} = -0.63$, and $k_{22} = -1.15$. The TV uncertainty covariance matrix is $\hat{\Sigma}_w^{\text{TV}} = \text{diag}(0.44, 0.09)$ and the sensor noise follows $\Sigma^{\text{sens}} = \text{diag}(0.25, 0.25, 0.028, 0.028)$ and $|w_{0,x}^{\text{sens}}| \leq 0.25$, $|w_{0,y}^{\text{sens}}| \leq 0.25$, $|w_{0,x}^{\text{sens}}| \leq 0.028$, $|w_{0,y}^{\text{sens}}| \leq 0.028$.

The safety parameters of Section V for the generation of TV safety rectangles and to distinguish between the cases are $\varepsilon_{\text{safe}} = 0.01$ m, $d_{\text{lar}} = 200$ m, $r_{\text{close}} = 90$ m, $r_{\text{close}}^{\text{FTP}} = \max\{10 \text{ m}, |v_0 N_{\text{FTP}} T|\}$, $v_{\text{LC, min}} = 10 \text{ m s}^{-1}$, and $\Delta s_{N, \text{min}} = 22.5$ m.

The weighting matrices of the SMPC and FTP optimal control problems (39) and (45) are $\mathbf{Q} = \text{diag}(0, 0.25, 0.2, 10)$, $\mathbf{R} = \text{diag}(0.33, 5)$, and $\mathbf{S} = \text{diag}(0.33, 15)$.

In all scenarios the initial EV reference is set to $[d_{\text{ref}}, \phi_{\text{ref}}, v_{\text{ref}}] = [0, 0, 27]$. While the reference orientation and velocity remain constant throughout the simulation, the reference lane is adapted depending on the current EV lateral position. The EV reference for the lateral position is always set to the current EV lane center.

Given this simulation setup, we now investigate the individual scenarios and analyze the proposed SMPC+FTP method.

B. Regular Highway Scenario

We first analyze a regular highway scenario. The initial states of the vehicles are given in Table I. The five TVs shown in Figure 7 all maintain their initial velocities and lanes,

TABLE I
INITIAL VEHICLE STATES

vehicle	initial state
EV	$[0, 0, 0, 27]^\top$
TV1	$[70, 20, 0, 0]^\top$
TV2	$[125, 20, 3.5, 0]^\top$
TV3	$[-245, 20, 0, 0]^\top$
TV4	$[-35, 32, 7, 0]^\top$
TV5	$[40, 32, 7, 0]^\top$

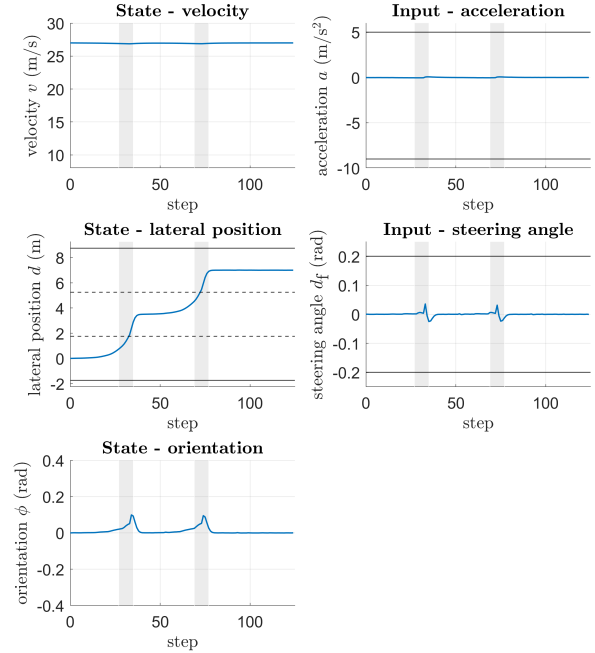


Fig. 8. SMPC+FTP states and inputs for the regular scenario. Vehicle motion in the gray areas is illustrated in Figure 9.

therefore, $\xi_{\text{ref},k}^{\text{TV}} = \xi_0^{\text{TV}}$. The initial longitudinal TV position is irrelevant in the computation of (11a).

In the following the SMPC+FTP solution is shown in detail and comparisons are made to an SMPC and an FTP method.

1) *SMPC+FTP*: Applying the proposed SMPC+FTP approach to the regular highway scenario yields efficient EV behavior in traffic. The SMPC risk parameter is chosen to be $\beta = 0.8$. The inputs and important states are shown in Figure 8. The gray areas in Figure 8 indicate selected sequences of the vehicle motion illustrated in Figure 9. The vehicle shapes are only shown for every second step to avoid overlapping of vehicle shapes in Figure 9. The EV approaches TV1 due to the velocity difference. The EV then changes lanes to the center lane with a moderate steering angle of $\delta < 0.04$. The center lane is approached with hardly any overshoot. Once TV2 is reached, the EV again changes lanes. As TV4 and TV5 are farther ahead, the EV smoothly moves to the left lane and eventually passes TV2. The vehicle orientation remains at a limited level, i.e., $\phi < 0.11$. Throughout the scenario, the EV maintains the reference velocity, and acceleration

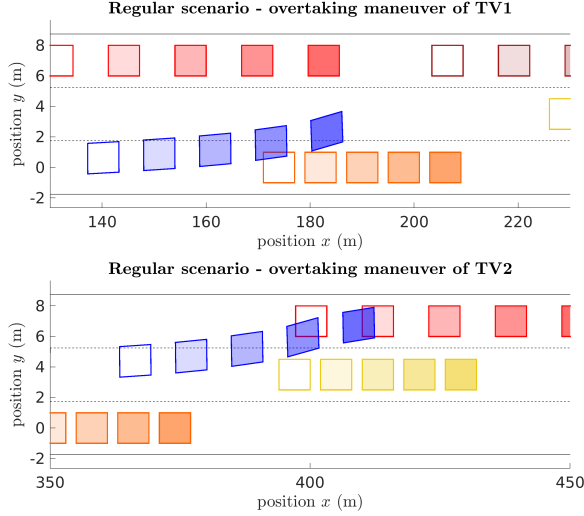


Fig. 9. Shots of the regular scenario with SMPC+FTP. Fading boxes show past states. The EV is shown in blue.

inputs are negligible. The average computation time to solve the SMPC and FTP optimal control problems are 0.11 s and 0.15 s, respectively. If applied in a setting that requires online computation, it would be possible that the computation cannot be performed successfully in the designated sample time period. This case is treated as if the FTP optimal control problem is infeasible. Therefore, the previously calculated, still valid safe input sequence would be used.

We will now take a closer look at the constraints for SMPC and FTP. SMPC constraints for time step $h = 22$ are illustrated in Figure 10 for two prediction steps, $k = 1$ and $k = 5$. The boxes represent the EV shape for the initial EV state and the TV safety rectangles at the given prediction step. The state of the current prediction step is marked with a bold cross, while other prediction steps are regular crosses. Initial vehicle states are indicated by a bold circle. For TV1 in the same lane as the EV, an inclined constraint is generated (case D). At each prediction step the constraint connects the initial EV shape with the TV1 safety rectangle at the predicted position. It is seen that the predicted SMPC trajectory for the EV stays above the constraint line. It is to note that only the respective predicted state must satisfy the illustrated constraint. Predicted states farther in the future satisfy respective constraints depending on a TV safety rectangle for a predicted TV position farther ahead. For TV2 case E is active, also resulting in an inclined constraint. Both TV4 and TV5 are two lanes left of the EV, yielding cases G and H, resulting in horizontal constraints to the right side of the TVs. TV3 is not shown in Figure 10 due to clarity as it is farther behind the other vehicles at this time instance.

The FTP constraints at step $h = 22$ for prediction steps, $k = 1$ and $k = 7$ are shown in Figure 11. The constraints are more conservative compared to the SMPC constraints. The reachable TV sets extend further to the back than the front, as maximal deceleration is larger than maximal acceleration. Additionally, the convex hull of reachable sets over two

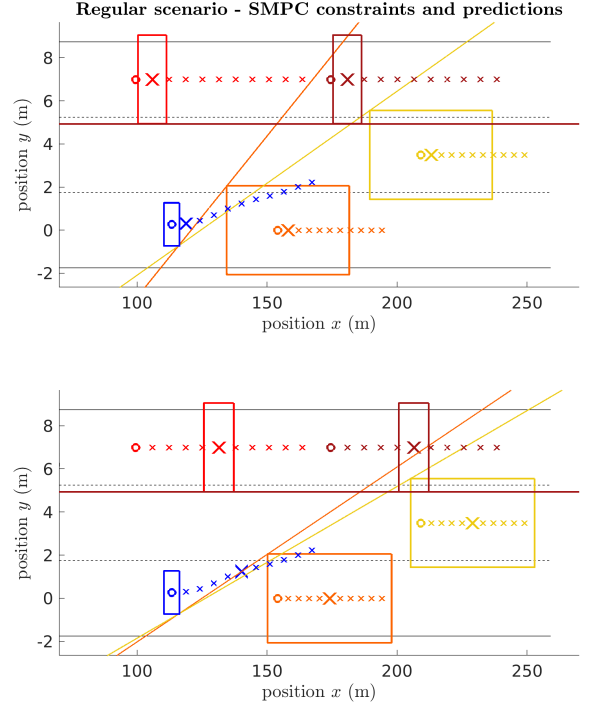


Fig. 10. SMPC constraints for the regular scenario at time step $h = 22$ and prediction steps $k = 1, k = 5$. The EV shape and planned trajectory are shown in blue. TVs as well as respective safety rectangles and constraints have the same color. Initial states are marked by a circle, the prediction step displayed is indicated by a bold cross, other predicted states are represented by smaller crosses.

consecutive steps is considered. Constraints for TV1 and TV2 are built according to cases D* and B*, respectively. Both constraints for TV4 and TV5 are generated given case H*. The planned SMPC trajectory is shown in dark blue for reference, while the FTP trajectory is shown in light blue. While the SMPC trajectory moves towards the center lane to overtake TV1, the FTP trajectory finds a vehicle motion which, for the final prediction step, remains in the current lane with $\phi = 0$ and enough distance to TV1, i.e., a safe terminal state. As the FTP optimal control problem yields a solution, i.e., a safe trajectory, the first input $u_{\text{SMPC},0}$ of the planned SMPC trajectory is then applied.

2) *Comparison to SMPC and FTP:* Throughout the entire simulation both the SMPC and FTP optimal control problems remain feasible. Therefore, the SMPC inputs are always applied. Only applying an SMPC algorithm without FTP would therefore yield the same result for this regular scenario.

Unlike SMPC, applying only FTP results in a different solution. As the constraints are more conservative compared to SMPC, the EV never changes lanes to overtake. As indicated by the FTP prediction in Figure 11, the FTP constraints keep the EV in its current lane. There are situations where the FTP solution leads to a lane change, however, these situations are rare and only occur to avoid an obstacle, not to actively overtake it.

We will use the following metric to compare the perfor-

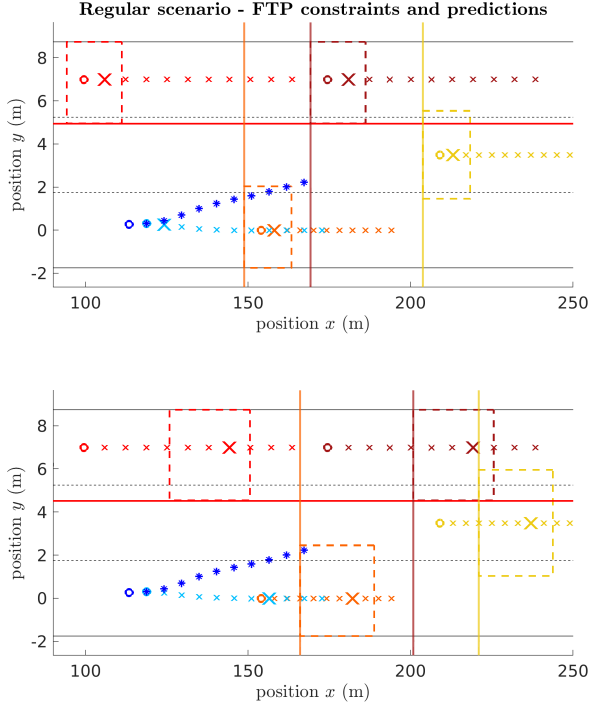


Fig. 11. FTP constraints for the regular scenario at time step $h = 22$ and prediction steps $k = 1, k = 7$. The EV is shown in blue. TVs as well as respective reachable sets and constraints have the same color. Initial states are marked by a circle. The initial FTP state starts after the first SMPC input is applied. The prediction step displayed is indicated by a bold cross, other predicted states are represented by smaller crosses. For reference, the planned SMPC trajectory is given by dark blue asterisks with a dark blue circle indicating the initial EV state.

mance of SMPC+FTP and FTP. Based on the cost function of the optimal control problem, the applied inputs and resulting states for the entire simulation are analyzed according to

$$J_{\text{sim}} = \sum_{k=1}^{N_{\text{sim}}} \|\Delta \xi_k\|_Q + \|u_{k-1}\|_R + \|\Delta u_{k-1}\|_S \quad (46)$$

with the simulation steps N_{sim} .

The overall cost for SMPC+FTP is $J_{\text{sim}} = 11.32$, while the overall FTP cost is $J_{\text{sim}} = 4.03\text{e}4$. As expected, the cost comparison shows that the SMPC+FTP approach yields a more efficient behavior than a safe FTP approach. In this case increased efficiency results from keeping the velocity close to the reference velocity.

3) *Risk Parameter Variation*: In the previously discussed simulation, the risk parameter was chosen to be $\beta = 0.8$. Here, we briefly analyze the effect of varying risk parameters on the EV performance. The risk parameters analyzed range from $\beta = 0.8$ to $\beta = 0.999$. The overall simulation cost, according to (46), for each risk parameter is given in Table II. Intuitively one could expect increasing cost with higher risk parameters. The overall costs of the simulation results show that the SMPC behavior and costs for a regular scenario are very similar. However, it can be beneficial regarding the cost to choose a larger risk parameter. While this slightly increases

TABLE II
RISK PARAMETER ANALYSIS

risk parameter β	0.8	0.9	0.95	0.99	0.999
cost J_{sim}	11.21	11.35	11.58	11.34	11.31

conservatism, inputs are changed more smoothly. In all five examples the EV behavior is almost similar.

4) *Varying Simulation Settings*: In the previous analysis, only one vehicle configuration is considered. In order to show that the SMPC+FTP method is suitable for various scenarios, we ran 1000 simulations, each consisting of 125 simulation steps, with randomly selected initial vehicle positions and velocities for each simulation run. The EV is located on one of the three lanes, i.e., $d_0 \in \{0, 3.5, 7\}$, with initial longitudinal position $s_0 = 0$ and velocity $v = 27$. The five TVs are randomly placed on one of the three lanes with an initial longitudinal position $x_0^{\text{TV}} \in [-100, 200]$, constant velocity $v_x^{\text{TV}} \in [20, 32]$, and constant $v_y^{\text{TV}} = 0$. It is ensured that all vehicles positioned on the same lane have an initial longitudinal distance $\Delta x \geq 50$ and that TV velocities are chosen such that TVs do not collide with each other. The SMPC+FTP method successfully handled all 1000 simulation runs and no collisions occurred.

C. Emergency Highway Scenario

After having shown the efficient SMPC+FTP planning for a regular highway scenario, we now illustrate the safety property of the proposed algorithm in an emergency scenario. The initial vehicle states are the same as in the regular scenario, see Table I. However, in this emergency scenario the TVs change their velocities and lateral positions. Starting at time step $h = 20$ TV5 initiates an emergency braking maneuver with maximal deceleration until reaching a complete halt. This causes TV4 to change lanes to the center lane in order to avoid TV5. TV1 reduces its velocity to $v_x^{\text{TV1}} = 10 \text{ m s}^{-1}$. After having passed TV5, TV4 moves to the left lane to then pass the slower TV2. TV1 also increases its velocity to $v_x^{\text{TV1}} = 20 \text{ m s}^{-1}$.

In the following SMPC without FTP is analyzed first. Then the solution of the proposed SMPC+FTP algorithm is presented.

1) *SMPC*: Applying only SMPC results in optimistic EV trajectory planning, while not considering highly unlikely events. Even though TV4 is slowly moving to the center lane, the EV still moves to the center lane to overtake TV1, as the predicted collision probability with TV4 remains below the specified risk parameter. However, at step $h = 25$ TV4 continues to increase its lateral velocity towards the center lane and TV1 decreases its velocity, therefore disallowing the EV to return to the right lane. There exists no feasible solution to the SMPC optimal control problem anymore which satisfies the chance constraint with the desired risk parameter. This causes the EV to collide with TV4 due to the concatenation of multiple unlikely and disregarded events. The collision sequence is illustrated in Figure 12. While SMPC performs well

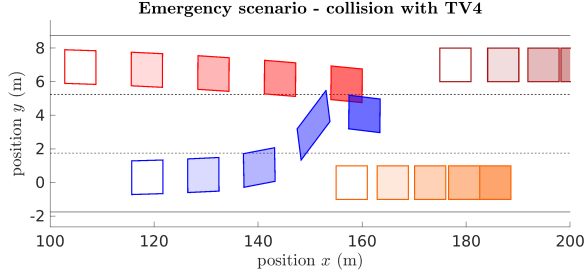


Fig. 12. Shots of the emergency scenario collision applying only SMPC. Fading boxes show past states. The EV is shown in blue.

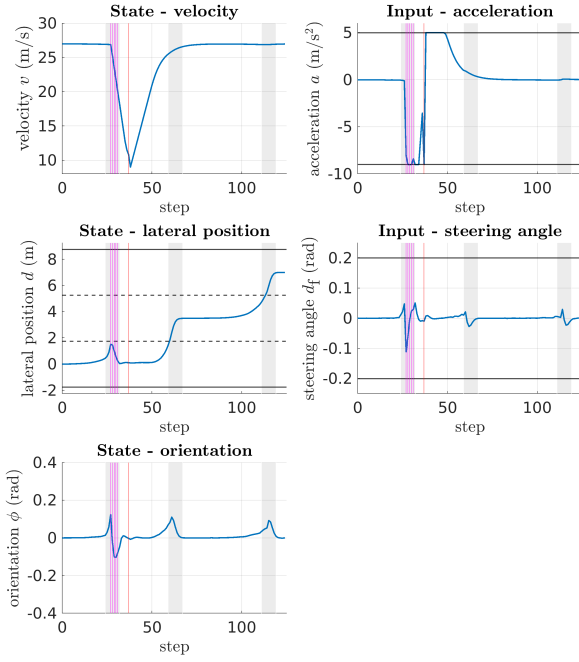


Fig. 13. SMPC+FTP states and inputs for the emergency scenario. Pink vertical lines represent infeasible SMPC and feasible FTP solutions, red vertical lines show infeasible FTP solutions. Vehicle motion in the gray areas is illustrated in Figure 14.

in regular scenarios without unlikely uncertainty realizations, these rare situations cause major safety issues.

2) *SMPC+FTP*: We now show how the proposed SMPC+FTP method handles the emergency scenario. The EV states and inputs are given in Figure 13. Gray areas represent sequences illustrated in Figure 14.

Initially the EV attempts to switch lanes and overtake TV1. However, at step $h = 27$ the SMPC is unable to find a solution. The FTP problem is still solved successfully and the first planned FTP input is applied. For the next four steps the SMPC optimal control problem remains infeasible, indicated by the pink lines in Figure 13, and the FTP inputs are applied, which are obtained by successfully solving the FTP OCPs. The EV slows down and returns to the right lane, as illustrated in the first shot of Figure 14. At step $h = 37$ the SMPC problem is feasible and the EV plans to overtake TV1 again. However, as TV4 is still too close, the FTP is unable to

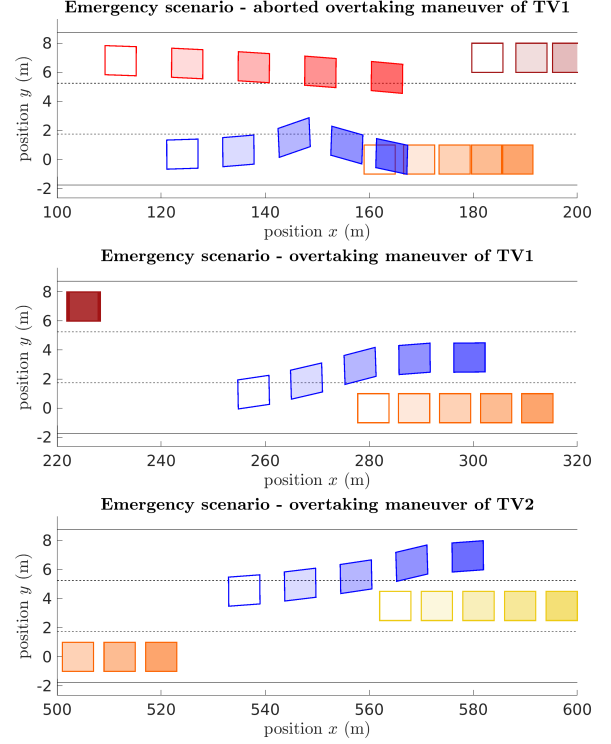


Fig. 14. Shots of the emergency scenario with SMPC+FTP. Fading boxes show past states. The EV is shown in blue.

find a new safe backup trajectory if the next planned SMPC input were applied, i.e., the FTP OCP becomes infeasible. Therefore, while the SMPC problem is still feasible, the safe input sequence obtained at the previous time step $h = 36$ is applied to the EV, as indicated by the red line in Figure 13. The EV remains in the right lane until TV4 is far enough away to safely change to the center lane. Eventually the EV passes TV2 by smoothly switching to the left lane with a small steering angle change. The average computation time for solving the SMPC and FTP optimal control problems are 0.15 s and 0.22 s, respectively. The values are higher compared to the regular scenario, as the computation time for infeasible optimal control problems is significantly larger.

In this rare emergency situation, the EV inputs lead to a less smooth motion. However, this is acceptable as safety is guaranteed even in this challenging situation.

It is also possible to only apply FTP in this emergency scenario. While this leads to safe vehicle behavior throughout the simulation, the EV does not overtake TV1 and TV2. The combination of SMPC and FTP, however, enables the EV to safely handle this emergency scenario while passing slower TVs when possible. Comparing the cost yields the following result. Applying FTP to the emergency scenario yields a cost of $J_{\text{sim}} = 4.28\text{e}4$, while the SMPC+FTP cost is $J_{\text{sim}} = 3.34\text{e}4$.

The SMPC and FTP constraints at step $h = 24$ and prediction step $k = 4$ closely before the aborted lane change maneuver are displayed in Figure 15. Whereas the SMPC

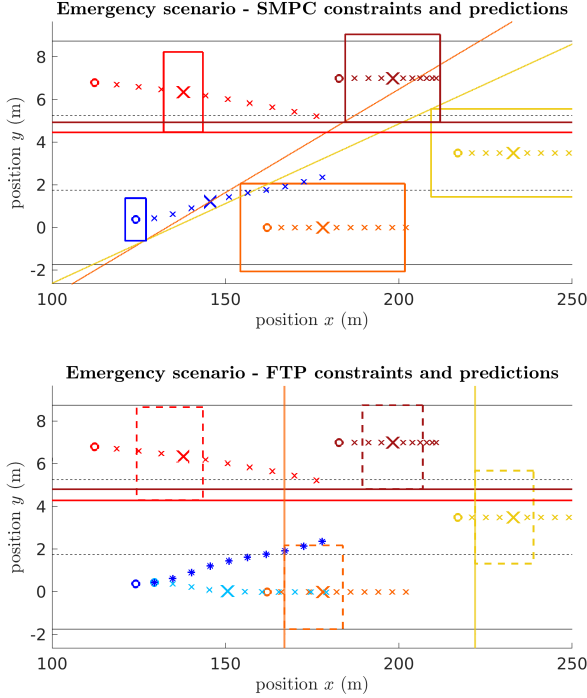


Fig. 15. SMPC+FTP constraints for the emergency scenario at time step $h = 24$ and prediction step $k = 4$. SMPC constraints are illustrated in the top, FTP constraints in the bottom. The EV shape and planned trajectory are shown in blue. TVs as well as respective safety rectangles, reachable sets, and constraints have the same color. Initial states are marked by a circle. The initial FTP state starts after the first SMPC input is applied. The prediction step displayed is indicated by a bold cross, other predicted states are represented by smaller crosses. For reference, in the FTP plot the planned SMPC trajectory is given by dark blue asterisks with a dark blue circle indicating the initial EV state.

prediction plans to steer the EV into the center lane, the planned FTP trajectory remains in the right lane. Once the FTP is unable to still find a safe trajectory remaining in the right lane, given the first SMPC step $u_{\text{SMPC},0}$, the FTP takes control.

In summary, the simulation scenarios in this section have shown the benefits of the proposed SMPC+FTP method. The SMPC part optimistically plans trajectories which are executed as long as there always exists a safe backup trajectory, computed by FTP. In regular scenarios SMPC+FTP provides benefits known from SMPC. In emergency scenarios the safety guarantee of FTP holds while the EV is still more efficient compared to applying pure FTP.

VII. DISCUSSION

In MPC applications, the prediction horizon is a design choice. While in general long prediction horizons are useful, here it is beneficial to select a relatively short SMPC horizon. This decreases the chance of the SMPC problem becoming infeasible and it is not necessary to employ a long horizon, as FTP is used to guarantee safety. In some FTP approaches it is required that the vehicle comes to a standstill at the end of the fail-safe trajectory. Here, we only require a certain

distance to vehicles ahead and zero orientation offset with respect to the road for the terminal state. This enables the use of a relatively short FTP horizon. However, if the FTP horizon is selected too short, lane changes are not possible anymore, as the FTP requires a certain amount of prediction steps to fulfill the terminal constraint. For very short FTP horizons lane change maneuvers are therefore aborted before the lane change actually takes place.

It is possible to get oscillating behavior between applied SMPC inputs and the activation of FTP. In other words, in step one the SMPC input is applied, which potentially causes the FTP to intervene in the next step. Then, a safe state is again achieved, leading to another, potentially over-aggressive SMPC input, again requiring FTP in the subsequent step. This can be avoided by designing the SMPC controller and its constraints less aggressively, as done in the simulation study.

Regarding the simulation, simulating each scenario once is adequate. While the TV is assumed to behave probabilistically by the EV, the actual TV behavior here is deterministic. And whereas SCMP depends on drawn samples, which vary between simulations, the applied SMPC approach uses a chance constraint reformulation that always yields the same constraint, given the same uncertainty distribution.

In the emergency scenario multiple TVs change velocities or lanes. This scenario was chosen such that the SMPC method causes a collision, which usually does not happen even for highly unlikely TV trajectories. The chance constraint within SMPC does allow a small probability of constraint violation, however, in most cases the iterative structure of MPC handles potential future constraint violations. Furthermore, constraint violations do not necessarily cause collisions, as the safety area around a TV is larger than the actual TV shape.

Comparing the planned SMPC trajectories for the EV at two consecutive time steps without any major environment changes, one would assume that the planned trajectory remains similar. However, this is not the case. The constraints with respect to other TVs are generated based on the EV state at the beginning of the optimal control problem in order to formulate linear constraints. Therefore, in the next step, the constraint generation is based on an updated initial EV state, resulting in a slightly different planned SMPC trajectory compared to the previously planned trajectory. This could be addressed by using EV predictions for the constraint generation, however, this would require nonlinear constraints.

The applied vehicle inputs in the emergency scenario lead to relatively high steering angles. This is not ideal for a smooth vehicle motion. Even though this behavior is acceptable in rare cases, the motion could be optimized by defining more cases for the constraint generation.

The individual SMPC and FTP algorithms in this work are possible controller realizations, specifically designed for highway scenarios with multiple TVs. The properties of the combined SMPC+FTP method are not restricted to the suggested SMPC and FTP trajectory planners described in Section V-A and Section V-B, respectively. Other SMPC or FTP approaches can be applied.

In dense traffic or unclear traffic situations, humans often do not wait until the desired vehicle motion is entirely realizable.

Instead, humans often slowly initiate maneuvers, causing other vehicles to react. For example, cutting into a lane is often preceded by slight motion towards the other lane so that other vehicles leave extra space. Therefore, it is possible to execute the lane change maneuver successfully, even though it was not possible to safely plan the entire lane change maneuver initially. While perfectly mimicking this human approach by automated vehicles is challenging due to safety reasons, the proposed SMPC+FTP framework enables automated vehicle motion that comes close to this efficient human behavior.

VIII. CONCLUSION

In this work we presented a safe and efficient SMPC+FTP method for self-driving vehicles. While SMPC is used to plan optimistic, efficient vehicle trajectories, a fail-safe trajectory planning (FTP) MPC problem ensures that only those SMPC inputs are applied which keep the vehicle in a safe state. The advantages of the proposed SMPC+FTP algorithm are shown in a simulation study, where comparisons are done to pure SMPC and pure FTP methods.

The efficiency of the SMPC+FTP method depends on the proposed constraint generation. Extending and refining the case differentiation will have a positive effect on efficiency. Considering urban automated driving, the SMPC+FTP approach remains valid, however, the case differentiation must be adapted to fit the urban traffic environment.

The presented SMPC+FTP method is suitable to be applied to further safety-critical transportation applications, such as currently developed air taxis. However, it is also possible to extend the application area to non-transportation applications, such as human-robot collaboration, where uncertainty is always present while safety must still be guaranteed.

APPENDIX A LINEARIZED AND DISCRETIZED SYSTEM MATRICES

The linearized, time-discrete system matrices A_d and B_d in (6) are given by

$$A_d = \begin{bmatrix} 1 & 0 & -Tv \sin z_1 & Tv \cos z_1 - \frac{z_2 \sin z_1}{2z_4} \\ 0 & 1 & Tv \cos z_1 & Tv \sin z_1 + \frac{z_2 \cos z_1}{2z_4} \\ 0 & 0 & 1 & \frac{T \tan \delta}{z_4} \\ 0 & 0 & 0 & 1 \end{bmatrix} \quad (47a)$$

$$B_d = \begin{bmatrix} \frac{T^2 \cos z_1}{2} & -\frac{T^2 v z_7 \sin z_1}{2} - \frac{\sin z_1}{z_4} \\ \frac{T^2 \sin z_1}{2} & \frac{T^2 v z_7 \cos z_1}{2} + \frac{z_8 \cos z_1}{z_4} \\ \frac{T^2 \tan \delta}{2z_4} & T z_7 \\ T & 0 \end{bmatrix} \quad (47b)$$

with

$$z_1 = \phi + \arctan \left(\frac{l_r \tan \delta}{l_r + l_f} \right) \quad (48a)$$

$$z_2 = T^2 v \tan \delta \quad (48b)$$

$$z_3 = (l_r \tan \delta)^2 \quad (48c)$$

$$z_4 = (l_r + l_f) \frac{z_3}{\sqrt{(l_r + l_f)^2 + 1}} \quad (48d)$$

$$z_5 = v \left((\tan \delta)^2 + 1 \right) \quad (48e)$$

$$z_6 = (l_r + l_f)^3 \left(\frac{z_3}{(l_r + l_f)^2 + 1} \right)^{\frac{3}{2}} \quad (48f)$$

$$z_7 = \frac{z_5}{z_4} - \frac{z_3 z_5}{z_6} \quad (48g)$$

$$z_8 = T l_r z_5. \quad (48h)$$

APPENDIX B PROOF OF THEOREM 1

Proof. Recursive feasibility is proved by induction by showing that $\Gamma_h \neq \emptyset \Rightarrow \Gamma_{h+1} \neq \emptyset$ for all $h \in \mathbb{N}$.

At time step $h = 0$ it holds that $\chi_0^{U_{\text{safe}, \text{init}}} \in \Gamma_0$, i.e., an initially safe trajectory exists according to Assumption 4. If at step $h = 0$ the FTP OCP can be solved, a new safe input set $U_{\text{safe}, 0}$ is obtained according to (14) or (15). This new safe input set $U_{\text{safe}, 0}$ remains valid at step $h = 1$ and ensures that a safe trajectory exists, i.e., $\chi_1^{U_{\text{safe}, 0}} \in \Gamma_1$. If at step $h = 0$ the FTP OCP is infeasible, the shifted previous safe input set remains valid, i.e., $U_{\text{safe}, 0} = U_{\text{safe}, \text{init}}^{\leftarrow}$ according to Section IV-A3. In this case the shifted safe input set $U_{\text{safe}, 0} = U_{\text{safe}, \text{init}}^{\leftarrow}$ guarantees that $\chi_1^{U_{\text{safe}, 0}} \in \Gamma_1$. Therefore, $\Gamma_0 \neq \emptyset \Rightarrow \Gamma_1 \neq \emptyset$.

For $h = 1$ it holds that $\chi_1^{U_{\text{safe}, 0}} \in \Gamma_1$. A feasible FTP OCP yields the new safe input sequences $U_{\text{safe}, 1}$, such that there exists a safe trajectory $\chi_2^{U_{\text{safe}, 1}} \in \Gamma_2$. If the FTP OCP is infeasible, reusing the still valid previous safe input set $U_{\text{safe}, 0}$, i.e., setting $U_{\text{safe}, 1} = U_{\text{safe}, 0}^{\leftarrow}$, ensures that $\chi_2^{U_{\text{safe}, 1}} \in \Gamma_2$.

For time step $h \geq 2$ it holds that $\chi_h^{U_{\text{safe}, h-1}} \in \Gamma_h$. If the FTP OCP is feasible, this yields the new safe input sequences $U_{\text{safe}, h}$, such that there exists a safe trajectory $\chi_{h+1}^{U_{\text{safe}, h}} \in \Gamma_{h+1}$. If the FTP OCP is infeasible, the previous safe input set $U_{\text{safe}, h-1}$ is still valid and choosing $U_{\text{safe}, h} = U_{\text{safe}, h-1}^{\leftarrow}$ ensures that $\chi_{h+1}^{U_{\text{safe}, h}} \in \Gamma_{h+1}$.

Therefore, $\chi_{h+1}^{U_{\text{safe}, h}} \in \Gamma_{h+1}$ holds for all $h \in \mathbb{N}$, i.e., the proposed method is safe and recursively feasible. \square

APPENDIX C PROOF OF LEMMA 1

Proof. As longitudinal and lateral motion are uncorrelated, the covariance matrix is given in terms of a block diagonal matrix

$$\Sigma_k^e = \begin{bmatrix} \Sigma_{x,k}^e & 0 \\ 0 & \Sigma_{y,k}^e \end{bmatrix}, \quad (49)$$

with

$$\Sigma_{x,k}^e = \begin{bmatrix} \sigma_{x,k}^2 & \sigma_{xv_x,k}^2 \\ \sigma_{xv_x,k}^2 & \sigma_{v_x,k}^2 \end{bmatrix}, \quad (50)$$

$$\Sigma_{y,k}^e = \begin{bmatrix} \sigma_{y,k}^2 & \sigma_{yv_y,k}^2 \\ \sigma_{yv_y,k}^2 & \sigma_{v_y,k}^2 \end{bmatrix},$$

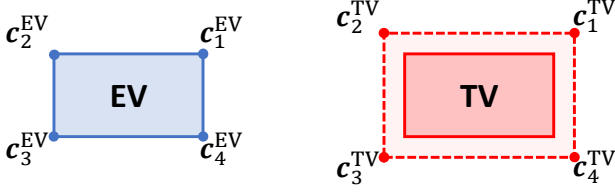


Fig. 16. Corner description for the EV shape and TV safety rectangle.

and each direction is computed independently. We will show that the error for the position coordinate x is distributed with a probability density function only depending on $\sigma_{x,k}^2$. Let $\xi_{x,k} = [x_k, v_{x,k}]^\top$ be the state vector projected onto its longitudinal coordinates with the estimated states $\hat{\xi}_{x,k} = [\hat{x}_k, \hat{v}_{x,k}]^\top$ and $e_{x,k} = \hat{\xi}_{x,k} - \xi_{x,k}$, then $e_{x,k}$ is Gaussian distributed with the bivariate probability function

$$f(e_{x,k}) = \frac{1}{2\pi\sqrt{\det(\Sigma_{x,k}^e)}} \exp\left(-\frac{1}{2}e_{x,k}^\top (\Sigma_{x,k}^e)^{-1} e_{x,k}\right). \quad (51)$$

We obtain the marginal probability density function by integrating $f(e_{x,k})$ over the longitudinal velocity, i.e.,

$$f_x(e_{x,k}) = \int_{-\infty}^{\infty} f(e_{x,k}) dv_{x,k}, \quad (52)$$

which yields

$$f_x(e_{x,k}) = \frac{1}{\sqrt{2\pi\sigma_{x,k}^2}} \exp\left(-\frac{1}{2\sigma_{x,k}^2}x_k^2\right). \quad (53)$$

As (53) corresponds to the univariate Gaussian distribution of the x -coordinate with only $\sigma_{x,k}$, the x -direction is computed independently of $\sigma_{v_{x,k}}$ and $\sigma_{xv_{x,k}}$, which proves the lemma. The same proof holds for the lateral direction. \square

APPENDIX D CONSTRAINT GENERATION

Here, we give a complete overview of the cases considered. The cases and conditions for SMPC are found in Table III. The values $c_{i,x/y,k}^{\text{EV/TV}}$, $i \in \{1, 2, 3, 4\}$ indicate the corner x -position and y -position of the EV shape or TV safety rectangle, according to Figure 16. While the main idea of the cases is already given in Section V-A4, some extra details were not previously mentioned for clarity. The function f_{close} was considered to be a simple constant, however, the full function consists of a constant part r_{close} and a variable part $\max\{0, \text{sign}(\Delta v) \Delta v N \Delta t\}$, i.e., the necessary distance between the EV and TV depends on the velocity difference. A larger velocity difference results in greater difference of distance covered by the EV and TV within the prediction time $N \Delta t$. This yields

$$f_{\text{close}} = r_{\text{close}} + \max\{0, \text{sign}(\Delta v) \Delta v N \Delta t\}. \quad (54)$$

As the general plan for the EV is to overtake only on the left, case E is extended slightly compared to Section V-A4. When the EV is too close to the TV, based on a left-lane margin

r_{lim} , a vertical constraint behind the TV replaces the inclined constraint (case E₃). It is only planned to overtake TVs on a lane left of the EV if the EV velocity is larger than the TV velocity (case E₂). For cases D and E the constraint slope is bounded such that it does not lie within with the EV shape or the TV safety rectangle.

The cases and conditions for FTP are similar to the SMPC cases. A complete description is given in Table IV. The main idea of the FTP cases are described in Section V-B2. Here, we give a detailed description of the cases where three placeholder TV predictions are considered (cases J* and C*). The cases with a TV prediction in the same lane as the EV are denoted by J_S*, C_S*, while cases with a TV prediction in a lane to the left or right of the TV are denoted by J_L*, C_L* and J_R*, C_R*, respectively. The slopes for cases C_L* and C_R* are limited to $q_{x,k} \leq 0$ and $q_{x,k} \geq 0$, respectively. If the values for $q_{x,k}$ exceed the respective limits, the cases C_{L,lim}* and C_{R,lim}* are applied. The cases F₂* and H₂* represent scenarios where the EV center is not in the TV lane, but the EV shape is already in the TV lane. In these cases, where the EV is behind the TV, vertical constraints behind the TV are built. The cases F* and H* are split into F_a*, F_b* and H_a*, H_b*, respectively.

ACKNOWLEDGMENT

The authors thank Daniel Althoff, Matthias Althoff, and Christian Pek for valuable discussions.

REFERENCES

- [1] M. Keller, C. Hass, A. Seewald, and T. Bertram. Driving simulator study on an emergency steering assist. In *International IEEE Conference on Systems, Man, and Cybernetics, San Diego, California/USA*, pages 3008–3013, 2014.
- [2] J. Levinson, J. Askeland, J. Becker, J. Dolson, D. Held, S. Kammel, J. Z. Kolter, D. Langer, O. Pink, V. Pratt, M. Sokolsky, G. Stanek, D. Stavens, A. Teichman, M. Werling, and S. Thrun. Towards fully autonomous driving: Systems and algorithms. In *2011 IEEE Intelligent Vehicles Symposium (IV)*, pages 163–168, Baden-Baden, Germany, June 2011.
- [3] C. Katrakazas, M. Quddus, W. Chen, and L. Deka. Real-time motion planning methods for autonomous on-road driving: State-of-the-art and future research directions. *Transportation Research Part C: Emerging Technologies*, 60:416–442, 2015.
- [4] D.Q. Mayne. Model predictive control: Recent developments and future promise. *Automatica*, 50(12):2967 – 2986, 2014.
- [5] R. Soloperto, J. Köhler, F. Allgöwer, and M. A. Müller. Collision avoidance for uncertain nonlinear systems with moving obstacles using robust model predictive control. In *2019 18th European Control Conference (ECC)*, pages 811–817, 2019.
- [6] S. Dixit, U. Montanaro, M. Dianati, D. Oxtoby, T. Mizutani, A. Mouza-kitis, and S. Fallah. Trajectory planning for autonomous high-speed overtaking in structured environments using robust mpc. *IEEE Transactions on Intelligent Transportation Systems*, 21(6):2310–2323, 2020.
- [7] A. Mesbah. Stochastic model predictive control: An overview and perspectives for future research. *IEEE Control Systems*, 36(6):30–44, Dec 2016.
- [8] M. Farina, L. Giulioni, and R. Scattolini. Stochastic linear model predictive control with chance constraints – a review. *Journal of Process Control*, 44(Supplement C):53 – 67, 2016.
- [9] A. Carvalho, Y. Gao, S. Lefevre, and F. Borrelli. Stochastic predictive control of autonomous vehicles in uncertain environments. In *12th International Symposium on Advanced Vehicle Control*, Tokyo, Japan, 2014.
- [10] G. Cesari, G. Schildbach, A. Carvalho, and F. Borrelli. Scenario model predictive control for lane change assistance and autonomous driving on highways. *IEEE Intelligent Transportation Systems Magazine*, 9(3):23–35, Fall 2017.

TABLE III
SMPC CONSTRAINTS

case	longitudinal conditions (pos. and vel.)	lateral conditions (pos.)	$q_{x,k}$	$q_{y,k}$	$q_{t,k}$
A	$ \Delta x_0^{\text{EV,TV}} \geq r_{\text{lar}}$	-	0	0	0
B	$f_{\text{close}} < -(\Delta x_0^{\text{EV,TV}}) < r_{\text{lar}}$	-	1	0	$-c_{2,x,k}^{\text{TV}}$
C	$f_{\text{close}} < (\Delta x_0^{\text{EV,TV}}) < r_{\text{lar}}$	-	-1	0	$c_{1,x,k}^{\text{TV}}$
D	$0 \leq -(\Delta x_0^{\text{EV,TV}}) \leq f_{\text{close}}$	$y_{\text{lane},0}^{\text{EV}} = y_{\text{lane},0}^{\text{TV}}$	$\max\left\{0, \frac{c_{4,y,0}^{\text{EV}} - c_{2,y,k}^{\text{TV}}}{c_{4,x,0}^{\text{EV}} - c_{2,x,k}^{\text{TV}}}\right\}$	-1	$c_{2,y,k}^{\text{TV}} - s_{x,k} c_{4,x,0}^{\text{EV}}$
E	$-\left(\Delta x_0^{\text{EV,TV}}\right) \leq f_{\text{close}},$ $s_0 + 0.5w_{\text{veh}} + r_{\text{llm}} \leq x_0^{\text{TV}},$ $v_0 - v_{x,0}^{\text{TV}} > 0$	$y_{\text{lane},0}^{\text{EV}} + w_{\text{lane}} = y_{\text{lane},0}^{\text{TV}}$	$\max\left\{0, \frac{c_{4,y,0}^{\text{EV}} - c_{2,y,k}^{\text{TV}}}{c_{4,x,0}^{\text{EV}} - c_{2,x,k}^{\text{TV}}}\right\}$	-1	$c_{2,y,k}^{\text{TV}} - s_{x,k} c_{4,x,0}^{\text{EV}}$
E ₂	$-\left(\Delta x_0^{\text{EV,TV}}\right) \leq f_{\text{close}},$ $s_0 + 0.5w_{\text{veh}} + r_{\text{llm}} \leq x_0^{\text{TV}},$ $v_0 - v_{x,0}^{\text{TV}} > 0$	$y_{\text{lane},0}^{\text{EV}} + w_{\text{lane}} = y_{\text{lane},0}^{\text{TV}}$	1	0	$-c_{2,x,k}^{\text{TV}}$
E ₃	$0 \leq -(\Delta x_0^{\text{EV,TV}}) \leq f_{\text{close}},$ $s_0 + 0.5w_{\text{veh}} + r_{\text{llm}} > x_0^{\text{TV}}$	$y_{\text{lane},0}^{\text{EV}} + w_{\text{lane}} = y_{\text{lane},0}^{\text{TV}}$	0	1	$-c_{3,y,k}^{\text{TV}}$
F	$ \Delta x_0^{\text{EV,TV}} \leq f_{\text{close}}$	$y_{\text{lane},0}^{\text{EV}} > y_{\text{lane},0}^{\text{TV}}$	0	-1	$c_{2,y,k}^{\text{TV}}$
G	$0 \leq -(\Delta x_0^{\text{EV,TV}}) \leq f_{\text{close}}$	$y_{\text{lane},0}^{\text{EV}} + 2w_{\text{lane}} \leq y_{\text{lane},0}^{\text{TV}}$	0	1	$-c_{3,y,k}^{\text{TV}}$
H	$0 < (\Delta x_0^{\text{EV,TV}}) \leq f_{\text{close}}$	$y_{\text{lane},0}^{\text{EV}} \leq y_{\text{lane},0}^{\text{TV}}$	0	1	$-c_{4,y,k}^{\text{TV}}$
J	$0 < (\Delta x_0^{\text{EV,TV}}) \leq f_{\text{close}}$	$y_{\text{lane},0}^{\text{EV}} = y_{\text{lane},0}^{\text{TV}}$	0	0	0

- [11] S. Magdici and M. Althoff. Fail-safe motion planning of autonomous vehicles. In *2016 IEEE 19th International Conference on Intelligent Transportation Systems (ITSC)*, pages 452–458, 2016.
- [12] S. Söntges and M. Althoff. Computing the drivable area of autonomous road vehicles in dynamic road scenes. *IEEE Transactions on Intelligent Transportation Systems*, 19(6):1855–1866, 2018.
- [13] T. Brüdigam, M. Olbrich, D. Wollherr, and M. Leibold. Stochastic model predictive control with a safety guarantee for autonomous driving. *IEEE Transactions on Intelligent Vehicles*, pages 1–1, 2021.
- [14] C. Hubmann, J. Schulz, M. Becker, D. Althoff, and C. Stiller. Automated driving in uncertain environments: Planning with interaction and uncertain maneuver prediction. *IEEE Transactions on Intelligent Vehicles*, 3(1):5–17, 2018.
- [15] B. Mirchevska, C. Pek, M. Werling, M. Althoff, and J. Boedecker. High-level decision making for safe and reasonable autonomous lane changing using reinforcement learning. In *2018 21st International Conference on Intelligent Transportation Systems (ITSC)*, pages 2156–2162, 2018.
- [16] U. Rosolia, A. Carvalho, and F. Borrelli. Autonomous racing using learning model predictive control. In *2017 American Control Conference (ACC)*, pages 5115–5120, 2017.
- [17] J. Kabzan, L. Hewing, A. Liniger, and M. N. Zeilinger. Learning-based model predictive control for autonomous racing. *IEEE Robotics and Automation Letters*, 4(4):3363–3370, 2019.
- [18] A. Wischniewski, J. Betz, and B. Lohmann. A model-free algorithm to safely approach the handling limit of an autonomous racecar. In *2019 IEEE International Conference on Connected Vehicles and Expo (ICCVE)*, 2019.
- [19] T. Stahl, A. Wischniewski, J. Betz, and M. Lienkamp. Multilayer graph-based trajectory planning for race vehicles in dynamic scenarios. In *2019 IEEE Intelligent Transportation Systems Conference (ITSC)*, pages 3149–3154, 2019.
- [20] C. Massera Filho, M. H. Terra, and D. F. Wolf. Safe optimization of highway traffic with robust model predictive control-based cooperative adaptive cruise control. *IEEE Transactions on Intelligent Transportation Systems*, 18(11):3193–3203, 2017.
- [21] H. Kazemi, H. N. Mahjoub, A. Tahmasbi-Sarvestani, and Y. P. Fallah. A learning-based stochastic mpc design for cooperative adaptive cruise control to handle interfering vehicles. *IEEE Transactions on Intelligent Vehicles*, 3(3):266–275, 2018.
- [22] B. Gutjahr, L. Gröll, and M. Werling. Lateral vehicle trajectory optimization using constrained linear time-varying mpc. *IEEE Transactions on Intelligent Transportation Systems*, 18(6):1586–1595, June 2017.
- [23] B. Yi, P. Bender, F. Bonarens, and C. Stiller. Model predictive trajectory planning for automated driving. *IEEE Transactions on Intelligent Vehicles*, 4(1):24–38, 2019.
- [24] Y. Rasekhipour, A. Khajepour, S. Chen, and B. Litkouhi. A potential field-based model predictive path-planning controller for autonomous road vehicles. *IEEE Transactions on Intelligent Transportation Systems*, 18(5):1255–1267, 2017.
- [25] C. Pek and M. Althoff. Computationally efficient fail-safe trajectory planning for self-driving vehicles using convex optimization. In *2018 21st International Conference on Intelligent Transportation Systems (ITSC)*, pages 1447–1454, Nov 2018.
- [26] Jeremy H. Gillula. *Guaranteeing Safe Online Machine Learning via Reachability Analysis*. Dissertation, Stanford University, 2013.
- [27] B. Schürmann, N. Kochdumper, and M. Althoff. Reachset model predictive control for disturbed nonlinear systems. In *2018 IEEE Conference on Decision and Control (CDC)*, pages 3463–3470, 2018.
- [28] M. Althoff, D. Heß, and F. Gambert. Road occupancy prediction of traffic participants. In *16th International IEEE Conference on Intelligent Transportation Systems (ITSC)*, pages 99–105, 2013.
- [29] M. Althoff, M. Koschi, and S. Manzing. Commonroad: Composible benchmarks for motion planning on roads. In *2017 IEEE Intelligent Vehicles Symposium (IV)*, pages 719–726, Los Angeles, USA, 2017.
- [30] S. Manzing, C. Pek, and M. Althoff. Using reachable sets for trajectory planning of automated vehicles. *IEEE Transactions on Intelligent Vehicles*, pages 1–1, 2020.
- [31] A.T. Schwarm and M. Nikolaou. Chance-constrained model predictive control. *AICHE Journal*, 45(8):1743–1752, 1999.
- [32] L. Blackmore, M. Ono, A. Bektassov, and B.C. Williams. A probabilistic particle-control approximation of chance-constrained stochastic predictive control. *Trans. Rob.*, 26(3):502–517, June 2010.
- [33] D. Lenz, T. Kessler, and A. Knoll. Stochastic model predictive controller with chance constraints for comfortable and safe driving behavior of autonomous vehicles. In *2015 IEEE Intelligent Vehicles Symposium (IV)*, pages 292–297, Seoul, South Korea, 2015.
- [34] J. Suh, H. Chae, and K. Yi. Stochastic model-predictive control for lane change decision of automated driving vehicles. *IEEE Transactions on Vehicular Technology*, 67(6):4771–4782, June 2018.
- [35] G. Schildbach and F. Borrelli. Scenario model predictive control for

TABLE IV
FTP CONSTRAINTS

case	longitudinal conditions (pos. and vel.)	lateral conditions (pos.)	$q_{x,k}$	$q_{y,k}$	$q_{t,k}$
A*	$ \Delta x_0^{\text{EV,TV}} \geq r_{\text{lar}}$	-	0	0	0
B*	$f_{\text{close}}^{\text{FTP}} < -(\Delta x_0^{\text{EV,TV}}) < r_{\text{lar}}$	-	1	0	$-c_{2,x,k}^{\text{TV}}$
D*	$0 \leq -(\Delta x_0^{\text{EV,TV}}) \leq f_{\text{close}}^{\text{FTP}}$	$y_{\text{lane},0}^{\text{EV}} = y_{\text{lane},0}^{\text{TV}}$	1	0	$-c_{2,x,k}^{\text{TV}}$
F _a *	$0 < (\Delta x_0^{\text{EV,TV}}) \leq f_{\text{close}}^{\text{FTP}}$	$y_{\text{lane},0}^{\text{EV}} > y_{\text{lane},0}^{\text{TV}}$	0	-1	$c_{2,y,k}^{\text{TV}}$
F _b *	$0 \leq -(\Delta x_0^{\text{EV,TV}}) \leq f_{\text{close}}^{\text{FTP}}$	$y_{\text{lane},0}^{\text{EV}} > y_{\text{lane},0}^{\text{TV}},$ $d_0 \geq y_{\text{lane},0}^{\text{TV}} + 0.5w_{\text{lane}} + 0.5w_{\text{veh}}$	0	-1	$c_{2,y,k}^{\text{TV}}$
F ₂ *	$0 \leq -(\Delta x_0^{\text{EV,TV}}) \leq f_{\text{close}}^{\text{FTP}}$	$y_{\text{lane},0}^{\text{EV}} > y_{\text{lane},0}^{\text{TV}},$ $d_0 < y_{\text{lane},0}^{\text{TV}} + 0.5w_{\text{lane}} + 0.5w_{\text{veh}}$	1	0	$-c_{2,x,k}^{\text{TV}}$
H _a *	$0 < (\Delta x_0^{\text{EV,TV}}) \leq f_{\text{close}}^{\text{FTP}}$	$y_{\text{lane},0}^{\text{EV}} < y_{\text{lane},0}^{\text{TV}}$	0	1	$-c_{3,y,k}^{\text{TV}}$
H _b *	$0 \leq -(\Delta x_0^{\text{EV,TV}}) \leq f_{\text{close}}^{\text{FTP}}$	$y_{\text{lane},0}^{\text{EV}} < y_{\text{lane},0}^{\text{TV}},$ $d_0 \leq y_{\text{lane},0}^{\text{TV}} - 0.5w_{\text{lane}} - 0.5w_{\text{veh}}$	0	1	$-c_{3,y,k}^{\text{TV}}$
H ₂ *	$0 \leq -(\Delta x_0^{\text{EV,TV}}) \leq f_{\text{close}}^{\text{FTP}}$	$y_{\text{lane},0}^{\text{EV}} < y_{\text{lane},0}^{\text{TV}},$ $d_0 > y_{\text{lane},0}^{\text{TV}} - 0.5w_{\text{lane}} - 0.5w_{\text{veh}}$	1	0	$-c_{2,x,k}^{\text{TV}}$
J _S *	$0 < (\Delta x_0^{\text{EV,TV}}) \leq f_{\text{close}}^{\text{FTP}}$	$y_{\text{lane},0}^{\text{EV}} = y_{\text{lane},0}^{\text{TV}}$	-1	0	$c_{1,x,k}^{\text{TV}}$
J _L *	$0 < (\Delta x_0^{\text{EV,TV}}) \leq f_{\text{close}}^{\text{FTP}}$	$y_{\text{lane},0}^{\text{EV}} = y_{\text{lane},0}^{\text{TV}}$	0	1	$-c_{4,y,k}^{\text{TV}}$
J _R *	$0 < (\Delta x_0^{\text{EV,TV}}) \leq f_{\text{close}}^{\text{FTP}}$	$y_{\text{lane},0}^{\text{EV}} = y_{\text{lane},0}^{\text{TV}}$	0	-1	$-c_{1,y,k}^{\text{TV}}$
C _S *	$f_{\text{close}}^{\text{FTP}} < (\Delta x_0^{\text{EV,TV}}) < r_{\text{lar}}$	$y_{\text{lane},0}^{\text{EV}} = y_{\text{lane},0}^{\text{TV}}$	-1	0	$c_{1,x,k}^{\text{TV}}$
C _L *	$f_{\text{close}}^{\text{FTP}} < (\Delta x_0^{\text{EV,TV}}) < r_{\text{lar}}$	$y_{\text{lane},0}^{\text{EV}} = y_{\text{lane},0}^{\text{TV}}$	$\frac{c_{3,y,0}^{\text{EV}} - c_{1,y,k}^{\text{TV}}}{c_{3,x,0}^{\text{EV}} - c_{1,x,k}^{\text{TV}}}$	-1	$c_{1,y,k}^{\text{TV}} - s_{x,k} c_{3,x,0}^{\text{EV}}$
C _{L,lim} *	$f_{\text{close}}^{\text{FTP}} < (\Delta x_0^{\text{EV,TV}}) < r_{\text{lar}}$	$y_{\text{lane},0}^{\text{EV}} = y_{\text{lane},0}^{\text{TV}}$	-1	0	$c_{1,x,k}^{\text{TV}}$
C _R *	$f_{\text{close}}^{\text{FTP}} < (\Delta x_0^{\text{EV,TV}}) < r_{\text{lar}}$	$y_{\text{lane},0}^{\text{EV}} = y_{\text{lane},0}^{\text{TV}}$	$-\frac{c_{2,y,0}^{\text{EV}} - c_{4,y,k}^{\text{TV}}}{c_{2,x,0}^{\text{EV}} - c_{4,x,k}^{\text{TV}}}$	1	$-(c_{4,y,k}^{\text{TV}} - s_{x,k} c_{2,x,0}^{\text{EV}})$
C _{R,lim} *	$f_{\text{close}}^{\text{FTP}} < (\Delta x_0^{\text{EV,TV}}) < r_{\text{lar}}$	$y_{\text{lane},0}^{\text{EV}} = y_{\text{lane},0}^{\text{TV}}$	1	0	$-c_{4,x,k}^{\text{TV}}$

lane change assistance on highways. In *2015 IEEE Intelligent Vehicles Symposium (IV)*, pages 611–616, Seoul, South Korea, 2015.

- [36] M.C. Campi and S. Garatti. A sampling-and-discarding approach to chance-constrained optimization: Feasibility and optimality. *Journal of Optimization Theory and Applications*, 148(2):257–280, Feb 2011.
- [37] G. Schildbach, L. Fagiano, C. Frei, and M. Morari. The scenario approach for stochastic model predictive control with bounds on closed-loop constraint violations. *Automatica*, 50(12):3009 – 3018, 2014.
- [38] T. Brüdigam, M. Olbrich, M. Leibold, and D. Wollherr. Combining stochastic and scenario model predictive control to handle target vehicle uncertainty in autonomous driving. In *2018 21st IEEE International Conference on Intelligent Transportation Systems (ITSC)*, pages 1317–1324, 2018.
- [39] T. Brüdigam, F. di Luzio, L. Pallottino, D. Wollherr, and M. Leibold. Grid-based stochastic model predictive control for trajectory planning in uncertain environments. In *2020 IEEE 23rd International Conference on Intelligent Transportation Systems (ITSC)*, pages 1–8, 2020.
- [40] S. Steyer, G. Tanzmeister, and D. Wollherr. Grid-based environment estimation using evidential mapping and particle tracking. *IEEE Transactions on Intelligent Vehicles*, 3(3):384–396, Sep. 2018.
- [41] S. Steyer, C. Lenk, D. Kellner, G. Tanzmeister, and D. Wollherr. Grid-based object tracking with nonlinear dynamic state and shape estimation. *IEEE Transactions on Intelligent Transportation Systems*, pages 1–20, 2019.
- [42] J. Kong, M. Pfeiffer, G. Schildbach, and F. Borrelli. Kinematic and dynamic vehicle models for autonomous driving control design. In *2015 IEEE Intelligent Vehicles Symposium (IV)*, pages 1094–1099, Seoul, South Korea, 2015.
- [43] L. Grüne and J. Pannek. *Nonlinear Model Predictive Control*. Springer-Verlag, London, 2017.